PREPARATION, SURFACE FUNCTIONALIZATION AND APPLICATIONS OF CELLULOSE NANOCRYSTALS: A REVIEW

XINER LI

School of Materials Science and Engineering, Jiangsu University, Zhenjiang 212013, Jiangsu, P.R. China
✉ *Corresponding author: X. Li, 3230706058@stmail.ujs.edu.cn*

Received July 23, 2026

Cellulose nanocrystals (CNCs) are crystalline cellulose nanoparticles that commonly exhibit rod-like or needle-like shapes, although spherical morphologies are also reported. They are valued for their high stiffness, optical behaviour, biocompatibility and biodegradability. This review examines physical, chemical, biological and hybrid preparation routes, including high-pressure homogenization, ultrasonication, grinding, hydrolysis, oxidation, ionic liquids and deep eutectic solvents. It further discusses surface functionalization through non-covalent assembly, small-molecule covalent reactions, polymer grafting, cationization and supramolecular engineering. Representative applications in composite reinforcement, photonic materials, sensing, biomedicine, environmental remediation, tribology and food-related systems are critically compared. Particular attention is given to preparation–structure–performance relationships, hybrid isolation strategies and adaptive supramolecular networks. Remaining challenges associated with the energy and water demand of CNC manufacture and process scale-up, as well as their surface heterogeneity, long-term performance and material standardization are finally identified.

Keywords: cellulose nanocrystals, preparation methods, surface functionalization, hybrid processes, supramolecular engineering

INTRODUCTION

The growing concern about resource consumption, and environmental awareness have brought the high-value utilization of biomass to the centre of materials research. The objective is not merely to produce lightweight or mechanically robust materials, but to combine multiple functions within lower-carbon manufacturing routes. Cellulose is an attractive candidate as it is the most abundant natural polymer, is renewable and biocompatible, and has a hydroxyl-rich surface that can be chemically tailored without replacing the molecular backbone. These features have sustained both academic and industrial interest in cellulose-based materials.

Cellulose nanocrystals (CNCs) are a major class of nanocellulose produced by selectively removing disordered regions from natural cellulose, while retaining most crystalline domains. Their appeal arises from their high axial stiffness, low thermal expansion, large specific surface area, and hydroxyl-rich surfaces. CNCs can also self-assemble into chiral nematic liquid-crystalline structures, producing optical behaviour unavailable in conventional cellulose fibres. Nevertheless, the transition from laboratory suspensions to reliable materials remains challenging because the preparation route, surface charge, particle dimensions, and interparticle association jointly affect performance. This review therefore examines CNC structure, preparation, surface functionalization, and representative applications, with emphasis on preparation–structure–performance relationships.

Within the extensive literature on CNC preparation, modification and applications, the distinctive emphasis of this review lies in the connection between isolation conditions, the resulting particle geometry and surface chemistry, and the requirements of the final material. Physical, chemical, biological and hybrid routes are compared using these relationships, with particular attention to the trade-offs among colloidal stability, thermal resistance, resource demand and further functionalization. The discussion then links permanent surface modification with supramolecular and dynamic

covalent networks to explain how processing choices enable reinforcement, self-assembly and adaptive behaviour. This integrated perspective supports application-oriented selection of preparation and functionalization strategies. Figure 1 provides an overview of the review.

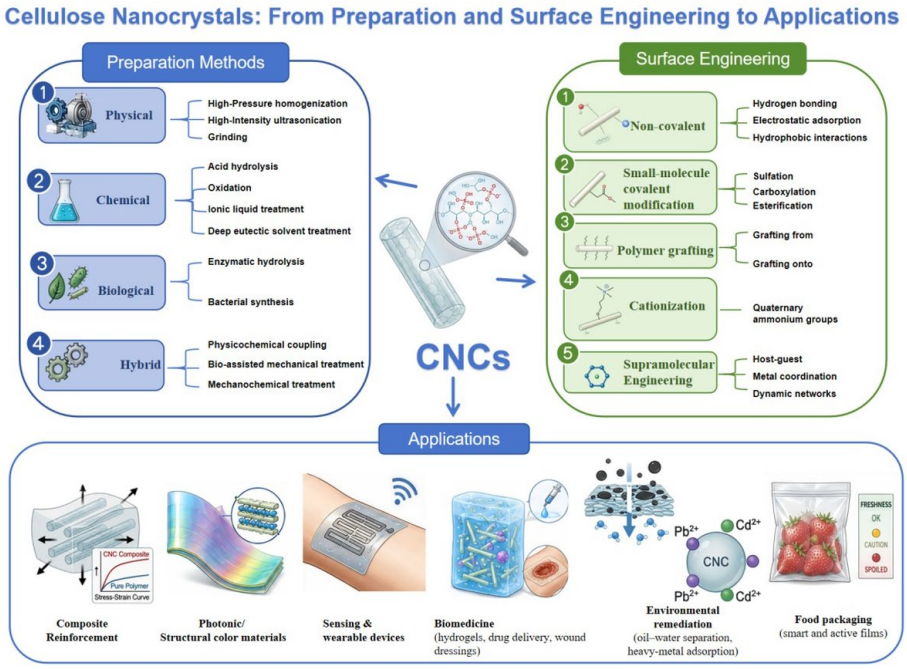


Figure 1: Overview of research on CNCs

STRUCTURAL CHARACTERISTICS AND CORE PROPERTIES OF CNCs

CNC performance is not governed by a single structural parameter. Particle geometry, crystal structure, surface chemistry and interparticle association act together, while their relative importance changes during processing and application. A material may, for example, have high crystallinity but poor dispersibility, or a high surface-charge density but limited thermal stability. CNCs usually exhibit rigid rod-like or needle-like morphologies, as illustrated in Figure 2 (a,b), and their dimensions depend strongly on cellulose source, pretreatment, and isolation method. Wood- and cotton-derived CNCs are commonly 100–500 nm long and 3–20 nm in diameter, with aspect ratios of approximately 5–30.[1–2] Extending the hydrolysis time of waste cotton reduced the CNC length and diameter from 195.6 and 6.6 nm after 30 min to 100.1 and 5.7 nm after 90 min, respectively.[3] By contrast, CNCs derived from tunicates or bacterial cellulose may retain lengths of 1000–1500 nm owing to their more continuous crystalline domains, resulting in higher aspect ratios.[1,4] Spherical CNCs with diameters of approximately 24–76 nm can also be produced by routes such as high-concentration enzymatic hydrolysis or high-temperature oxidation, as shown in Figure 2(c).[5–7] Spherical morphology is not restricted to a single isolation route: Fattahi Meyabadi *et al*. reported spherical cellulose nanoparticles from waste cotton through enzymatic hydrolysis followed by sonication, while retaining the crystalline cellulose structure.[8] Flores-Ramírez *et al.* also reported spherical cellulose nanoparticles as carriers for carminic acid.[9] These examples show that an exclusively rod-like definition is too restrictive; particle shape and crystalline structure should be characterized separately.

CNCs isolated from natural cellulose, including those produced by sulfuric-acid hydrolysis, generally retain the cellulose I polymorph, in which the molecular chains are arranged in parallel.[1] Their crystallinity is typically above 70% and can reach 95% or more under suitable conditions.[10–11] Strong alkaline treatment (mercerization) or prolonged hydrolysis may convert cellulose I into cellulose II, a thermodynamically more stable polymorph with antiparallel chain packing.[1,12] The nanoscale dimensions and high aspect ratio of CNCs provide a large specific surface area and facilitate the formation of interconnected or percolating

networks in polymer matrices, thereby improving reinforcement and barrier performance.

The physical properties of CNCs are closely related to these structural features. CNCs are among the strongest naturally derived nanomaterials; their estimated axial tensile strength is 2–6 GPa and their Young's modulus is approximately 150 GPa, values comparable to those of high-performance fibres such as Kevlar.[2,13] CNCs also exhibit a low thermal expansion coefficient (approximately 0.1 ppm K^{-1}) and good dimensional stability. Their thermal degradation behaviour, however, depends strongly on surface functionality. Sulfate half-ester groups can catalyse dehydration during heating and reduce the onset of degradation to approximately 200–250 °C, well below that of native cellulose.[11] Optically, aqueous CNC suspensions above a critical concentration of roughly 3–5 wt% can spontaneously form chiral nematic phases and display iridescent structural colour. The helical pitch is sensitive to surface-charge density, ionic strength, and external fields. Prolonged ultrasonication may increase the pitch and red-shift the reflected colour, whereas electrolyte-induced charge screening can reduce the pitch and blue-shift the reflection.

CNC surface chemistry largely determines colloidal stability, interfacial behaviour, and functionalization potential. Native CNC surfaces are rich in hydroxyl groups, while different isolation and modification routes introduce additional charged functionalities. Sulfuric-acid hydrolysis forms sulfate half-esters ($–OSO_3^-$), which generate electrostatic repulsion and improve aqueous dispersion. Sulfated CNCs commonly have zeta potentials below −30 mV; reported values of −26.1 to −46.1 mV indicate that a greater negative magnitude generally corresponds to stronger electrostatic stabilization.[14] CNCs extracted from green-tea residues reached a zeta potential of −58.49 mV and showed high colloidal stability in water.[15] Strongly negative zeta potentials are not exclusive to sulfation. TEMPO-mediated oxidation selectively converts C6 primary hydroxyl groups into carboxylates, producing a high and adjustable surface-charge density and enhanced dispersion stability.[16] Sulfate and carboxylate groups therefore stabilize CNC suspensions by a similar electrostatic mechanism but differ in thermal stability, chemical reactivity, and subsequent modification options. CNCs are also amphiphilic and can adsorb irreversibly at oil–water interfaces to form rigid protective layers in Pickering emulsions.[10,17] Their abundant surface hydroxyl groups provide reactive sites for diverse and targeted functionalization.

The rheology of CNC suspensions is central to processing and shaping. For predominantly rod-like CNCs, particle anisotropy and strong interparticle interactions promote concentration-dependent ordered networks, and suspensions can evolve from isotropic dispersions at low concentration to liquid-crystalline or gel states at higher concentration. This transition controls viscosity, flow behaviour, and film-forming quality. Increasing CNC concentration promotes the transition from an isotropic phase to a birefringent liquid-crystalline phase and consequently affects self-assembly kinetics, film morphology, colour uniformity, and mechanical properties.[3] Concentrated CNC suspensions generally exhibit non-Newtonian shear-thinning behaviour, which facilitates extrusion, coating, and printing: the material flows under shear but can partially recover its viscosity or network after deposition.

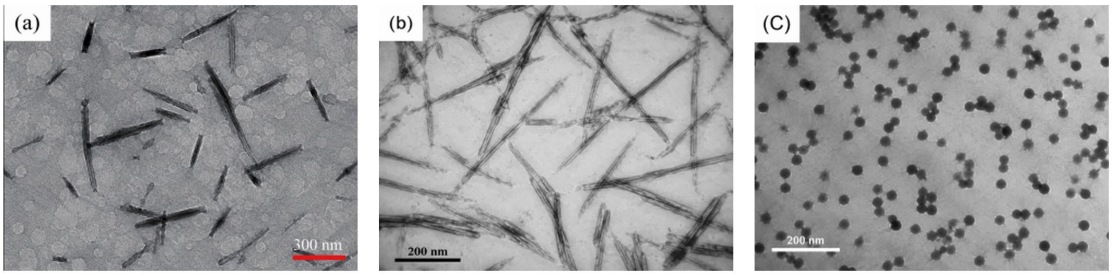


Figure 2: Rod-like (a), needle-like (b), and spherical (c) morphologies of CNCs (SEM images in panels (a–c) are original, acquired by the author, not reproduced from published literature)

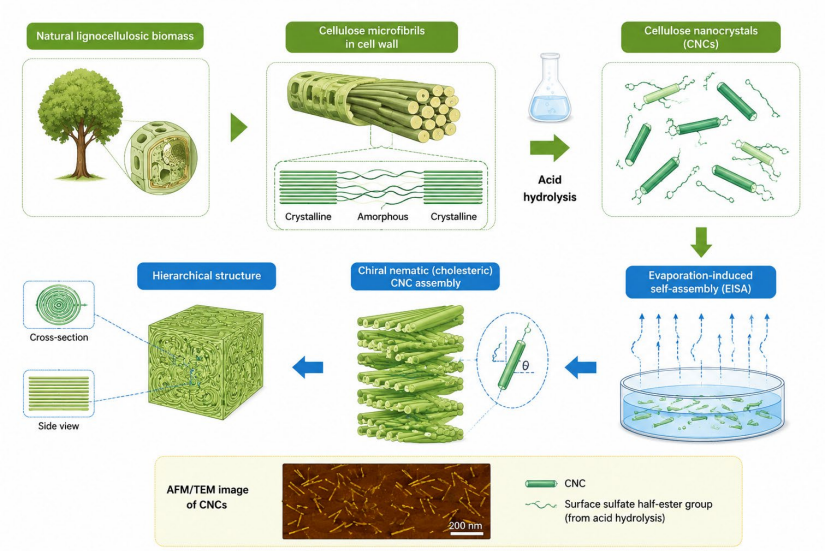


Figure 3: Flowchart of the CNC fabrication process

Similar behaviour has been observed in CNC-containing gels, in which higher CNC contents increased viscosity and strengthened three-dimensional networks through interfacial and electrostatic interactions.[15] Rheology therefore links nanoscale particle interactions to macroscopic processability and should be considered when designing CNC-based films, inks, hydrogels, coatings, and composites.

The biological performance of CNCs is also relevant to its functional applications. As biomass-derived materials, CNCs are renewable and potentially biodegradable, consistent with the principles of green chemistry and circular economy. Many studies report good biocompatibility and low cytotoxicity under appropriate exposure conditions, supporting their use in drug-delivery systems, tissue-engineering scaffolds, wound dressings, and biosensors. Nevertheless, biological responses remain dependent on dose, surface chemistry, impurities, and administration route.

METHODS FOR CNC PREPARATION

CNC isolation is fundamentally a selective deconstruction process. Amorphous or weakly ordered cellulose must be removed, cleaved, or loosened without excessive damage to the crystalline domains that are intended to remain. Physical, chemical, biological, and hybrid routes approach this task differently and therefore do not yield interchangeable materials. They alter aspect ratio, surface chemistry, yield, energy demand, and the composition of the waste stream. These differences are consequential because they determine the functions accessible to the resulting CNCs and motivate the continued development of lower-energy and lower-reagent preparation routes.[18] Figure 3 illustrates a representative sequence from lignocellulosic biomass to CNC isolation and subsequent chiral nematic self-assembly.

Physical methods

Physical methods use mechanical forces to disrupt the hydrogen-bonded structure of cellulose and can avoid much of the chemical contamination associated with acid or oxidative routes. Water is commonly used as the processing medium and few additional reagents are required, although low chemical consumption does not automatically imply low environmental impact because energy demand and throughput remain important constraints. High-pressure homogenization (HPH) is a representative example. A cellulose suspension is forced through a narrow valve at high pressure, generating intense shear, impact, and cavitation that loosen fibre bundles and promote longitudinal fibrillation. Because conventional HPH often retains amorphous material, it is commonly used as an auxiliary treatment; nevertheless, direct CNC isolation is possible under carefully controlled conditions. Park *et al.*[19] reported a chemical-free HPH route based mainly on temperature control. After 20 cycles, the resulting CNCs were 4–14 nm wide and 60–320 nm long, and crystallinity increased almost linearly with processing temperature. Repeated homogenization, however,

increases electricity consumption, processing time, equipment wear, and heat-management requirements. Scale-up therefore requires fewer passes, higher solids loading, effective blockage control, and energy-saving pretreatment. Aguado *et al.*[20] found that additional homogenization cycles increased the specific surface area from 12.4 to 23.4 $m^2\ g^{-1}$, but at the cost of higher energy input. The value of HPH consequently depends on the balance among product quality, throughput, energy use, and equipment durability.

High-intensity ultrasonication acts primarily through acoustic cavitation. Cavitation bubbles generated in a liquid grow and collapse under alternating pressure, producing local shock waves and high-velocity microjets. The resulting shear can disrupt hydrogen bonding, fragment less ordered regions, and promote the release and dispersion of crystalline nanoparticles from fibre bundles. Ultrasonication can therefore refine cellulose and regulate CNC morphology and assembly. Duan *et al.*[1] reported that increasing ultrasonic treatment altered the pitch of CNC chiral nematic phases from 483 to 501 nm, producing a visible red shift. Yang *et al.*[21] compared acid hydrolysis, TEMPO oxidation, and high-intensity ultrasonication for nanocellulose isolated from corn husks. The ultrasonicated sample retained the cellulose-I structure and had an average diameter of 20.14 ± 4.32 nm, but it showed lower crystallinity and poorer dispersion stability than the TEMPO-oxidized material. Although the method is chemically simple, heat generation, scale-dependent cavitation, and low energy efficiency can limit large-scale implementation.

Mechanical grinding reduces cellulose dimensions through repeated impact, shear, and friction between the fibres and grinding media or discs. The imposed mechanical energy disrupts hydrogen bonding, shortens cellulose chains, and promotes the progressive delamination of fibre bundles. The process can be conducted in water without strong acids or alkalis and uses comparatively simple equipment, although long treatment times and high energy demand may restrict scale-up. Kang *et al.*[22] prepared CNCs by ball milling cellulose in water followed by centrifugation. The resulting particles were 3–10 nm in diameter and 120–400 nm in length, with a yield of approximately 20%. Because no harsh chemicals or organic solvents were used, the products retained thermal stability comparable to that of the starting cellulose.

Chemical methods

Chemical methods remain among the most widely used routes for CNC production. Unlike purely mechanical treatments, they selectively hydrolyse or oxidize less ordered cellulose regions and may simultaneously introduce new surface groups. These reactions are generally efficient and controllable, but they do not necessarily provide low-cost or low-impact processing. Reagent recovery, equipment corrosion, washing requirements, and wastewater treatment are therefore central practical constraints.

Acid hydrolysis method

Acid hydrolysis is one of the most established CNC preparation methods. Under controlled conditions, concentrated acids preferentially cleave β-1,4-glycosidic bonds in disordered cellulose regions while largely preserving the ordered crystalline domains. Hydronium ions (H_3O^+) catalyse bond cleavage in the more accessible amorphous regions, converting them into soluble sugars and releasing nanoscale crystalline particles.[14,23]

Sulfuric-acid hydrolysis is the most commonly used acid route, and a representative process is shown in Figure 4. Qi *et al.*[10] showed that extending hydrolysis from 60 to 120 min reduced the average particle size from 138.03 to 39.60 nm and the crystallinity from 89.84% to 75.42%, while increasing the surface sulfate content. Sulfuric-acid hydrolysis thus provides well-dispersed CNCs, but the introduced sulfate half-esters catalyse dehydration during heating and reduce thermal stability.

Hydrochloric-acid hydrolysis has been explored as an alternative to sulfuric acid. Duan *et al.*[1] reported that HCl-derived CNCs had relatively low surface-charge density; the resulting weak electrostatic repulsion favoured aggregation and precipitation and hindered the formation of stable chiral nematic phases. Because HCl hydrolysis does not introduce thermally labile sulfate groups, however, the resulting CNCs generally retain higher thermal stability.[2,24]

Organic-acid hydrolysis has attracted increasing attention because it can reduce equipment corrosion, wastewater-treatment demand, and the thermal-stability penalty associated with sulfate groups. Song *et al.*[25] used a sulfuric-acid/acetic-acid/deionized-water mixture (1:8:1) to hydrolyse cassava-pulp cellulose at 80 °C, producing CNCs bearing acetoxy and carbonyl groups with an average particle size of

approximately 80 nm. The suspension showed no visible precipitation after 30 days and retained higher thermal stability than CNCs prepared by conventional sulfuric-acid hydrolysis. Cherian *et al.*[26] compared several organic acids: oxalic-acid-derived CNCs had a crystallinity of 81.51% and a zeta potential of −34 mV, whereas acetic-acid-derived CNCs showed a crystallinity of 77.03% and a zeta potential of −16.2 mV. Organic-acid routes therefore often improve thermal stability, although colloidal charge and yield depend on the acid. Chen *et al.*[27] further showed that concentrated oxalic, maleic, and p-toluenesulfonic acids can be recovered by cooling crystallization. At 20 °C, approximately 95% of oxalic acid could theoretically be recovered from a 70 wt% solution, while maleic acid and p-toluenesulfonic acid reached recoveries of roughly 80% at higher initial concentrations. The practical benefit of organic acids therefore depends on solubility, crystallization conditions, and recovery efficiency.

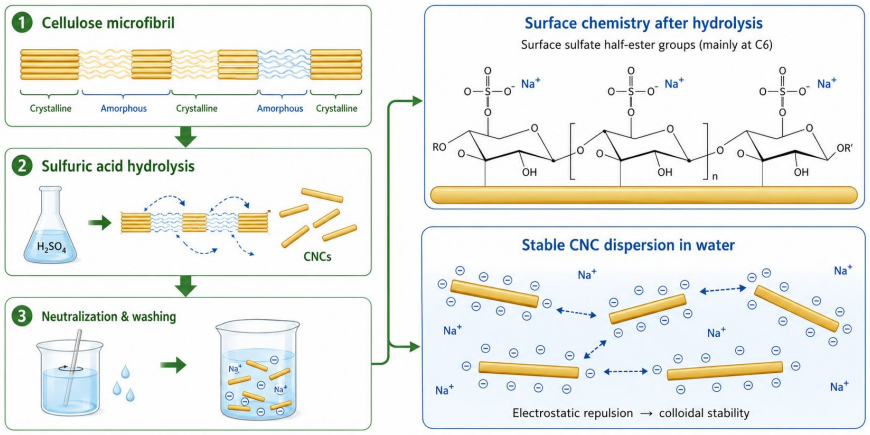


Figure 4: Isolation of CNCs from cellulose via sulfate hydrolysis

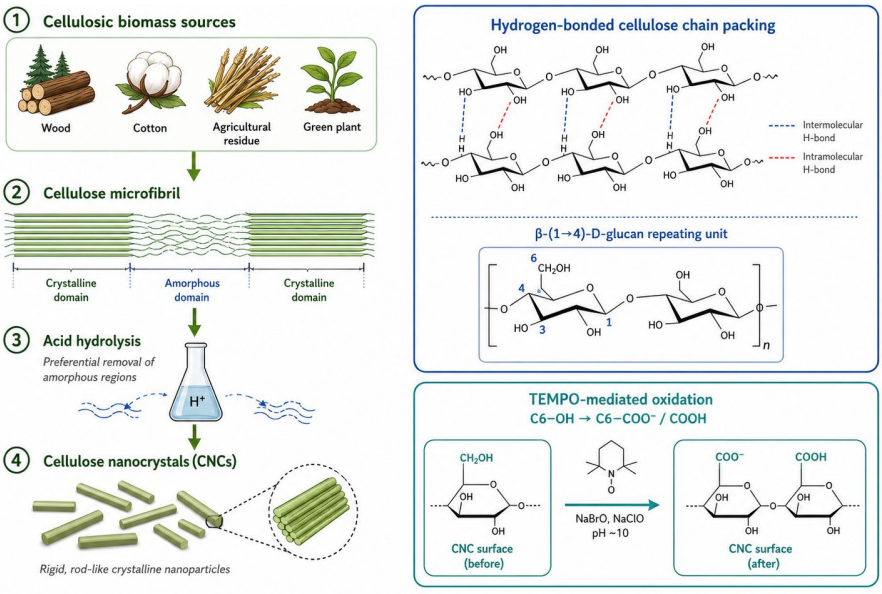


Figure 5: Preparation of CNCs via TEMPO oxidation and their chemical structures

Oxidation method

Oxidative routes selectively convert cellulose hydroxyl groups into carboxyl or aldehyde functionalities. Oxidation of accessible surface regions creates anionic groups that increase electrostatic repulsion and facilitate the dissociation of fibre bundles under mild mechanical treatment, such as low-energy ultrasonication. These routes can therefore combine nanoscale disintegration with direct control of surface chemistry.

TEMPO (2,2,6,6-tetramethylpiperidine-1-oxyl)-mediated oxidation is a widely studied route to carboxylated CNCs. In a typical TEMPO/NaBr/NaClO system, TEMPO acts as the catalyst and primary C6 hydroxyl groups are selectively oxidized to carboxylates. Fraschini *et al.*[16] used bleached softwood pulp in an alkaline TEMPO/NaBr/NaClO system and showed that the surface carboxyl density could be controlled by the NaClO dosage (Fig. 5). The resulting carboxylated CNCs had a zeta potential of −75 mV, indicating strong colloidal stabilization. Zhou *et al.*[28] combined TEMPO oxidation with ultrasonic cavitation under acid-free conditions. At a NaClO dosage of 10 mmol g^{-1}, the mass recovery reached 94% and the CNC width remained 3.5–3.6 nm with a narrow distribution. Unlike sulfate half-esters, carboxylate groups do not cause the same pronounced loss of thermal stability, although excessive oxidation can damage the crystalline domains.

Ammonium persulfate (APS) enables one-step oxidation and depolymerization. Thermal decomposition of APS produces sulfate radical anions ($SO_4^{\bullet-}$), which oxidize cellulose while promoting chain cleavage. Conventional APS treatment requires prolonged heating, whereas mechanochemical processing uses impact, shear, and friction to accelerate disintegration and oxidation. Lin *et al.*[29] applied Bayesian optimization to a mechanochemical process for carboxylated CNCs from microcrystalline cellulose. Bayesian optimization iteratively selected reaction temperature, oscillation frequency, time, ball-to-material ratio, liquid addition, and APS concentration to maximize yield and reduce resource use. Under the optimized conditions (60 °C, 30 Hz, 25 min, ball-to-material ratio 31.8, liquid addition 2 μL mg^{-1}, and APS concentration 0.5 M), the CNC yield was 90.45%, crystallinity was 78.26%, and average particle size was 196.15 ± 18.23 nm. Compared with solution-phase APS oxidation, the process shortened the reaction and reduced water and energy use. Its reproducibility, equipment wear, and scalability nevertheless require further evaluation.

Periodate oxidation provides a complementary route because $NaIO_4$ cleaves vicinal diols at the C2–C3 positions of anhydroglucose units to form dialdehyde groups. Zhao *et al.*[30] prepared uniformly needle-like periodate-oxidized CNCs (PO-CNCs) at 20 °C for 6 days under alkaline conditions (pH 10). The treatment also partially removed lignin, allowing high-purity products to be obtained from natural fibres such as flax without an additional bleaching step. The increased aldehyde functionality improves reactivity, although ring opening can reduce structural integrity if oxidation is excessive.

Ionic-liquid and deep-eutectic-solvent methods

The environmental burden and process complexity of conventional acid and oxidative methods have encouraged the use of alternative solvent systems. Ionic liquids (ILs) and deep eutectic solvents (DESs) are particularly attractive because their structures and solvent properties can be tuned, their vapour pressures are low, and they can potentially be recovered and reused.

ILs are low-melting-point salts composed of organic cations and organic or inorganic anions. Their strong hydrogen-bond-accepting ability can disrupt the intermolecular hydrogen-bond network of cellulose and enable dissolution or selective deconstruction. By controlling ion composition, temperature, and residence time, less ordered domains can be preferentially removed while crystalline regions are retained. Mariño *et al.*[31] reported a CNC yield of up to 70% using [Hmim][(HSO_4)(H_2SO_4)]. Life-cycle assessment estimated a production cost of US$0.81 g^{-1} and indicated lower climate-change and fossil-energy impacts than conventional acid hydrolysis when the solvent was recycled, although the high solvent cost remained a limitation.

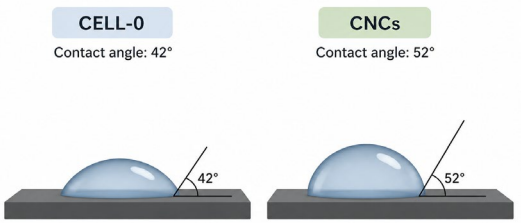


Figure 6: Water contact angles of cellulose and CNCs extracted from Angelim Vermelho wood (Cell-0), redrawn from data reported in Ref. [32]

Ionic liquids can also combine component separation with *in situ* surface functionalization. Abushammala *et al.*[32] treated wood flour directly with 1-ethyl-3-methylimidazolium acetate ([EMIM][OAc]) at 60 °C. After two cycles, 69% of lignin and 92% of hemicelluloses were removed. The treatment partially acetylated the CNC surface and increased the water contact angle from 42° to 52° (Fig. 6), indicating enhanced hydrophobicity. An ionic-liquid recovery of 95% reduced solvent consumption, although even small losses per cycle and the energy required for purification must be considered in industrial assessment.

DESs are eutectic mixtures formed through non-covalent interactions between hydrogen-bond donors and acceptors. Like ILs, they have tunable physicochemical properties and can compete with cellulose–cellulose hydrogen bonding, thereby loosening the association between ordered and disordered domains. Nicastro *et al.*[33] treated bleached eucalyptus pulp with a choline-chloride/oxalic-acid DES at 95 °C for 6 h and obtained a cellulose recovery of approximately 65%, compared with about 22% for the conventional sulfuric-acid route. Dialysis required roughly 2 days rather than more than 5 days, indicating improved resource utilization and shorter post-treatment. Lu *et al.*[34] prepared lignin-containing CNCs from peanut shells using an ultrasound-assisted ternary DES of choline chloride, guaiacol, and aluminium chloride hexahydrate (1:1:0.07) at 120 °C for 3 h. The cellulose content increased from 36.39% to 59.49%, while lignin and hemicellulose removals reached 73.22% and 93.05%, respectively. Subsequent ultrasonication produced needle-like LCNCs with 69.97% crystallinity and a maximum decomposition temperature of 337 °C. These results support DES processing of agricultural residues, but solvent composition, recovery, and product purification remain decisive for scale-up.

Biological methods

Physical methods avoid most chemical reagents, but can require substantial mechanical energy. Chemical routes are rapid and controllable, but create demands for reagent recovery, separation, and waste treatment. Biological routes operate under mild conditions and offer high molecular selectivity, although their reaction rates and productivity are generally lower.

Enzymatic hydrolysis

Enzymatic hydrolysis provides a mild route to CNCs through selective biocatalytic degradation. Specific enzymes preferentially attack accessible and disordered cellulose regions. Endoglucanases, for example, cleave β-1,4-glycosidic bonds within amorphous domains and can gradually release crystalline nanoparticles while preserving much of the ordered structure. Compared with strong-acid hydrolysis, this selectivity can improve thermal stability and reduce structural damage, but enzyme cost, reaction time, and product recovery remain important.

Jabalera *et al.*[35] treated filter paper with the ancestral endoglucanase LFCA_EG for 24 h at 40 °C and pH ≈ 6, producing enzymatic CNCs with an average length of 650 ± 390 nm. The addition of the fungal loosenin PcaLOOL12 weakened non-covalent interactions between microfibrils and improved enzyme accessibility. The average CNC length decreased to 250 ± 100 nm and the yield increased from 22.3% to 34.2%. The products retained a degradation temperature of 341–344 °C, compared with approximately 309 °C for sulfuric-acid-derived CNCs, demonstrating the benefit of enzymatic processing for preserving thermal stability.

Enzyme composition also provides a means of controlling CNC morphology. Tong *et al.*[6] showed that a system rich in endoglucanase (EG:xylanase = 9:1) favoured spherical or short rod-like CNCs, whereas a higher xylanase proportion (EG:xylanase = 1:9) produced longer rods with lengths approaching 1000 nm. Enzyme selection and ratio therefore regulate not only the reaction rate, but also the accessibility, fragmentation pattern, and final particle morphology.

Bacterial cellulose route

The bacterial-cellulose route uses microbially synthesized bacterial cellulose (BC) as a highly pure precursor. Cellulose-producing bacteria secrete BC during cultivation, after which acid or enzymatic hydrolysis is still required to remove less ordered regions and produce bacterial cellulose nanocrystals (BCNCs). Because BC contains little or no lignin and hemicelluloses, and has high crystallinity and structural uniformity, it is an attractive precursor for high-quality nanocrystals.[36] Thus, the route is bottom-up with respect to BC biosynthesis, but still includes a subsequent top-down deconstruction step for BCNC isolation.

Studies of this route often follow the structural evolution from BC membranes to bacterial cellulose nanofibres and finally to BCNCs. Arserim-Uçar *et al.*[37] produced BC membranes by static fermentation with *Acetobacter xylinum*, followed by alkaline treatment, mechanical disintegration, and freeze-drying to obtain nanofibres. Controlled sulfuric- or hydrochloric-acid hydrolysis then generated highly crystalline BCNCs. Increasing hydrolysis temperature and severity reduced particle size and increased crystallinity, while optimized conditions preserved thermal stability close to that of the original BC. The results demonstrate that nanoscale disintegration can be controlled without completely sacrificing the ordered structure.

Peña-Ortiz *et al.*[38] used an *Ancylobacter* sp. strain (STN1A) to produce bacterial nanocellulose from crude glycerol, a biodiesel by-product, and then adjusted the duration of sulfuric-acid hydrolysis. A 60 min treatment produced shorter BCNCs with an aspect ratio of 22.8, crystallinity of 63%, and zeta potential of −40.17 mV, whereas a 30 min treatment yielded longer particles with an aspect ratio of 26.9 and a zeta potential of −44.13 mV. This approach illustrates how fermentation feedstock and hydrolysis severity can be combined to tune particle dimensions, crystallinity, and colloidal stability while valorizing an industrial by-product.

Hybrid methods

No single preparation route resolves every processing constraint. Mechanical treatments can be chemically clean but energy intensive; chemical routes are efficient but reagent demanding; and enzymatic routes are selective but slow. Hybrid methods therefore combine two or more mechanisms, so that one step weakens the cellulose structure and a subsequent step completes nanoscale disintegration. Additional unit operations do not automatically make a process greener: their value must be demonstrated through milder conditions, shorter residence time, higher yield, or quantified reductions in reagent, water, or energy consumption.

Chemical–physical hybrid routes are among the most widely used strategies. Acid hydrolysis, oxidation, or ionic-liquid treatment first weakens the internal hydrogen-bond network or removes disordered cellulose, thereby reducing resistance to subsequent ultrasonication or high-pressure homogenization. Pang *et al.*[39] combined ultrasonic swelling in 1-butyl-3-methylimidazolium chloride (BmimCl) with low-concentration sulfuric-acid hydrolysis. The ionic-liquid pretreatment produced a swelling index of 82.2% and increased cellulose accessibility, enabling the subsequent acid concentration and processing severity to be reduced. The route improved CNC crystallinity and thermal stability, while decreasing acid demand and wastewater generation. Figure 7 schematically illustrates the role of ultrasonic pretreatment in an ionic-liquid-assisted preparation route.

Pretreatment efficiency is therefore central to hybrid processing. Haddis *et al.*[40] combined steam explosion with acid hydrolysis to isolate CNCs from poplar. The wood was treated for 5 min at 200 °C and 15.5 bar and then subjected to rapid depressurization. Hemicellulose removal and thermally induced chain rearrangement increased the crystallinity of the precursor to 1.3 times that of the untreated material, and the final CNC yield was 2.5 times higher. Particle size, crystallinity, and colloidal stability remained broadly comparable to those of CNCs from untreated poplar, while thermal stability improved. The example shows that structural preregulation can change the efficiency and outcome of subsequent hydrolysis rather than merely adding another processing step.

Bio–mechanical routes combine enzymatic selectivity with mechanical processing. Enzymatic removal of amorphous cellulose weakens fibre cohesion and can reduce the energy required for subsequent disintegration. Pereira and Arantes[41] integrated enzymatic CNC isolation at a high solids loading (>15 wt%) into a sugar-platform process for sugarcane bagasse. The resulting CNCs had diameters of approximately 20 nm, a yield of about 50%, and could be isolated without a costly high-energy ultrasonic dispersion step. Aguado *et al.*[20] further reported that enzymatic pretreatment reduced the energy demand of subsequent high-pressure homogenization by approximately 37% relative to purely mechanical processing. These results show that biological pretreatment can improve overall energy efficiency while preserving product quality. Mechanochemistry is another rapidly developing hybrid strategy. Ball milling creates a high-energy solid-state environment in which structural disintegration and chemical functionalization can occur simultaneously, avoiding some limitations of conventional dissolution–reaction–separation sequences. Lin *et al.*[29] reacted microcrystalline cellulose with 0.5 M APS at 60 °C for 25 min in a

ball-milling system and obtained carboxylated CNCs at a yield of 90.45%.

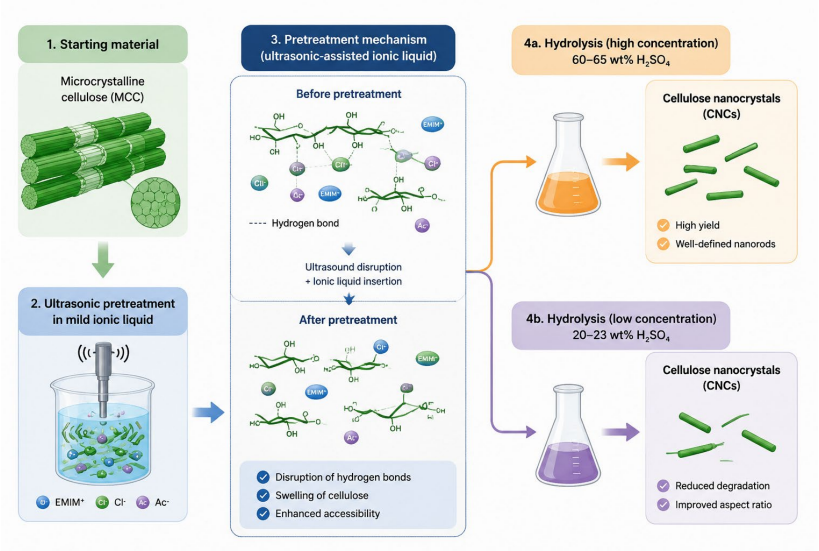


Figure 7: Schematic illustration of CNC preparation using ultrasonic pretreatment in an ionic liquid, based on the process reported in Ref. [39]

Relative to solution-phase APS oxidation, water consumption was reduced by nearly 60-fold and energy consumption by more than fourfold. Mechanochemistry therefore offers a resource-efficient route, although milling-media contamination, equipment wear, heat management, and scale-up require further attention.

Comparison of different preparation methods

The principal advantages and limitations of CNC preparation routes are compared in Table 1. No route is optimal for every application because isolation also determines the starting surface chemistry for subsequent functionalization. Sulfuric-acid hydrolysis provides electrostatic stabilization through sulfate half-esters, which is useful for aqueous processing and self-assembly, but these groups reduce thermal stability. Hydrochloric-acid and enzymatic routes avoid sulfation and can better preserve heat resistance, although additional stabilization may be needed. Oxidative routes provide carboxyl groups that support colloidal dispersion and subsequent coupling reactions, while excessive oxidation may damage the crystalline domains.[1,14,16,28,35]

Table 1
Comparison of CNC preparation routes

Category	Preparation method	Advantages	Disadvantages
Physical methods	High-pressure homogenization	High yield (>90%); requires minimal chemical reagents; suitable for large-scale production.	Extremely high energy consumption; the main product is cellulose nanofiber/cellulose nanofibril (CNF), which has low crystallinity; prone to equipment clogging, requiring pretreatment; the product has high viscosity.
	Ultrasound-assisted methods	Offer operational flexibility and can enhance the efficiency of chemical processes; allow for the control of chiral helical pitch and structural color; and deliver concentrated energy.	Have low energy efficiency, with a significant portion of energy converted into heat; consume high amounts of energy in large-scale applications and have limited processing capacity; and are relatively inefficient when used alone.

	Ball milling	Completely free of chemical reagents, using water as the sole medium, making it environmentally friendly; the process is simple, and post-processing is straightforward.	Extremely high energy consumption and long processing times; relatively low yield; over-milling can lead to a decrease in crystallinity.
Chemical methods	Sulfuric acid hydrolysis method	The process is well-established and has a short reaction time; the introduction of sulfate groups on the surface creates strong electrostatic repulsion, resulting in excellent dispersion in aqueous solutions; it offers high yields and high crystallinity.	Poor thermal stability (catalytic degradation of sulfate groups); generates large amounts of acidic wastewater, posing a significant environmental burden; equipment corrosion issues.
	Hydrolysis with hydrochloric acid	No surface charge is introduced, resulting in high thermal stability; chemical reagent costs are relatively low.	Due to the absence of surface charge, dispersion is poor, and aggregation and precipitation are likely; it is difficult to form a stable colloidal suspension.
	Organic acid hydrolysis method	Excellent thermal stability; organic acids are less corrosive and can be recovered and reused (recovery rate >95%), making the process environmentally friendly; the product exhibits good dispersibility.	The reaction requires higher temperatures (80–100°C) or longer reaction times; the yield is moderate; the surface charge density is lower than that of the sulfuric acid method.
	TEMPO oxidation method	High surface carboxyl group content, extremely high charge density (−40 to −75 mV), and excellent dispersibility; mild reaction conditions; good preservation of crystal structure.	TEMPO reagent is relatively expensive; post-treatment is required to remove nitrogen-containing byproducts; excess oxidizing agent can corrode the crystal core, reducing the yield.
	APS oxidation method	This one-pot method simultaneously achieves hydrolysis and oxidation; it can process lignin-containing feedstocks, simplifying the process; when combined with mechanochemical methods, it can significantly reduce reaction time.	Traditional methods have longer reaction times (16 h); conditions must be optimized to avoid over-oxidation; the thermal stability of the products is lower than that of enzymatic hydrolysis.
	Ionic liquid method	Solvent recovery and recycling (≥90%), environmentally friendly and sustainable; high crystallinity (up to 95% or higher); uniform product particle size.	Ionic liquids are relatively expensive; high viscosity limits mass transfer; moisture content must be precisely controlled.
Biological methods	Enzymatic hydrolysis	Mild conditions and high selectivity; no chemical contamination; excellent thermal stability (>340 °C); controllable product morphology.	Slow reaction rate and long cycle time (several hours to several days); moderate yield; relatively high enzyme costs; the product surface is nearly neutral, making it prone to

			agglomeration.
	Bacterial synthesis method	High purity (free of lignin and hemicellulose); unique three-dimensional network structure; product properties can be customized by adjusting hydrolysis conditions; utilizes industrial byproducts, aligning with the circular economy.	Long bacterial cultivation cycle (several weeks); low BNC yield (at the g/L level); requires subsequent acid hydrolysis to produce BCNCs, resulting in a lengthy process chain.

The comparison must also distinguish product yield from process efficiency. Mechanical treatment reduces dependence on chemical reagents, but can require substantial electricity and may yield fibrillar products unless the feedstock and conditions are carefully controlled. Ionic liquids and DESs offer tunable processing environments, but their practical value depends on solvent recovery, viscosity, purification and losses over repeated cycles. Enzymatic routes offer selectivity under mild conditions at the expense of reaction time and enzyme cost. Bacterial cellulose provides a pure precursor, but still requires cultivation and subsequent nanocrystal isolation.[19,20,31–35,37–38]

Hybrid routes can reduce the severity of individual steps by combining pretreatment with selective hydrolysis, oxidation or mechanical disintegration. Their advantage should be established using the complete process, including washing, separation and reagent recovery. Reported yields are not directly comparable when feedstocks, yield definitions and product-purity criteria differ. Selection should therefore begin with the required particle dimensions, crystallinity, surface groups and processing temperature, followed by assessment of throughput and total water, energy and reagent demand. These criteria connect preparation-method selection to the surface-functionalization strategies discussed below.[20,29,39–41]

SURFACE FUNCTIONALIZATION OF CNCs

Surface functionalization addresses a fundamental mismatch in CNC applications: the particles are reactive and strongly hydrophilic, whereas many target matrices and interfaces are comparatively nonpolar. Modification can therefore regulate adsorption, dispersion, interfacial affinity, and biological interactions, while preserving the crystalline core as much as possible.

Surface chemical modification

Surface chemical modification attaches functional molecules or polymers to CNCs through covalent or non-covalent interactions, thereby controlling interfacial properties, dispersion, and stimulus response. Hydroxyl, sulfate, and carboxyl groups provide reaction or adsorption sites for diverse surface architectures. The principal approaches considered here are physical adsorption and non-covalent assembly, small-molecule covalent modification, polymer grafting, and cationization.

Physical adsorption and non-covalent surface assembly

Physical adsorption and non-covalent assembly functionalize CNCs through hydrogen bonding, electrostatic attraction, van der Waals forces, hydrophobic association, ion exchange, and steric stabilization without forming new covalent bonds. These methods use mild conditions, preserve the crystalline cellulose framework, and are especially suitable for aqueous systems in which hydroxyl, sulfate, or carboxyl groups interact reversibly with polymers, surfactants, biomolecules, or oppositely charged modifiers.

Qi *et al.*[10] used pH-controlled electrostatic adsorption between negatively charged CNCs and quaternized lignin to build a dense interfacial layer that suppressed Pickering-emulsion coalescence. Kaboorani and Riedl[42] modified CNCs with hexadecyltrimethylammonium (HDTMA) through electrostatic adsorption and ion exchange, replacing inorganic counterions with quaternary-ammonium cations while introducing long alkyl chains. The treatment retained the cellulose-I crystal structure, improved dispersion in weakly alkaline organic media such as tetrahydrofuran, and strengthened compatibility with nonpolar polyester matrices. Hydrogen bonding with molecules such as polydopamine can similarly introduce radical-scavenging and ultraviolet-

screening functions, while cationic antibacterial molecules can be adsorbed without multistep covalent derivatization.[43]

End-capping-assisted redispersion is a related non-covalent strategy. During drying, adsorbed small molecules or polymers occupy surface hydroxyl sites and hinder the re-formation of a dense interparticle hydrogen-bond network. Niu *et al.*[44] used polyethylene glycol dimethyl ether as a capping agent; at 10 wt%, dried CNCs were completely redispersed within 2 h and retained good colloidal stability. Du *et al.*[45] combined maltodextrin (MDX) and sodium polyacrylate (PAAS). MDX competed for hydrogen bonding, while PAAS provided electrostatic repulsion; with 20% MDX and 0.3% PAAS, the redispersed particle-size distribution was nearly identical to that of the original suspension. The combined effects of hydrogen-bond shielding, steric hindrance, and electrostatic stabilization therefore improve CNC storage and reprocessing.

Small-molecule covalent modification

Small-molecule covalent modification introduces functional groups, such as carboxyl, thiol, alkyne, or vinyl moieties, through esterification, silanization, epoxide ring opening, amidation, Schiff-base formation, and related reactions.[43] Unlike physical adsorption, these reactions provide persistent surface functionality, although excessive substitution may damage the crystalline structure or reduce the availability of native hydroxyl groups.

Sulfation is one of the most common *in situ* surface modifications during CNC preparation. Concentrated sulfuric acid reacts with cellulose hydroxyl groups to form negatively charged sulfate half-esters ($–OSO_3^-$). Roman and Winter[46] established the importance of sulfate groups for aqueous colloidal stability and their adverse effect on thermal degradation. Qi *et al.*[10] showed that increasing the hydrolysis severity raised the surface sulfur content from 0.36 to 0.89 wt%, increased the magnitude of the zeta potential, and improved colloidal stability, while decreasing thermal stability. Thermogravimetric analysis by Beck-Candanedo *et al.*[47] likewise showed that sulfate groups initiate dehydration and degradation at lower temperatures. Sulfation therefore involves a clear trade-off: additional surface charge improves dispersion, but excessive sulfation is not universally beneficial because it compromises heat resistance.

Carboxylation selectively converts surface hydroxyl groups into carboxylates, increasing charge density, chemical reactivity, and metal-ion binding. Fraschini *et al.*[16] oxidized C6 primary hydroxyl groups in an alkaline TEMPO/NaBr/NaClO system and obtained carboxylated CNCs with a zeta potential of −75 mV. Zhao *et al.*[30] prepared needle-like PO-CNCs by alkaline periodate oxidation at 20 °C for 6 days, obtaining a zeta potential of −28.81 mV. Habibi *et al.*[48] emphasized that the structural consequences depend on the pathway: TEMPO oxidation is largely surface selective and can preserve the crystalline core, whereas periodate oxidation opens the anhydroglucose ring, increasing reactivity but potentially reducing structural integrity. The appropriate route must therefore balance functional-group density against retention of the crystal structure.

Esterification is an effective way to regulate CNC wettability and compatibility with hydrophobic matrices. Reaction of surface hydroxyl groups with anhydrides or organic acids introduces less polar substituents, lowers surface free energy, and improves interfacial adhesion. Gan *et al.*[49] varied the molar ratio of acetic anhydride to surface hydroxyl groups from 5:1 to 40:1 and increased the surface acetylation from 11.1% to 62.9%. At the highest level, compatibility with polyhydroxybutyrate improved and composite tensile strength increased by approximately 43%. Song *et al.*[25] introduced acetoxy groups directly during mixed sulfuric-acid/acetic-acid hydrolysis and obtained CNCs with improved thermal stability and no visible sedimentation after 30 days. Goussé *et al.*[50] showed that mild esterification primarily improves dispersion, whereas higher substitution or longer ester chains more strongly favour compatibility with hydrophobic polymers. Excessive substitution, however, can weaken the native hydrogen-bond network and reduce mechanical performance.

Polymer graft modification

Polymer grafting is commonly divided into “grafting onto” and “grafting from” strategies. In grafting onto, a pre-synthesized end-functional polymer is coupled to the CNC surface. In grafting from, an initiator or active site is first immobilized on the CNC and monomers are polymerized directly from the surface. Both approaches create a polymer layer that can improve compatibility and

introduce pH response, temperature response, adhesion, or other functions.[43]

Free-radical polymerization is a common grafting-from route. Zhang *et al.*[51] used ceric ammonium nitrate to generate radical sites on CNCs and initiated acrylic-acid polymerization, producing PAA-grafted CNCs. The surface carboxyl content reached 21.38 mmol g^{-1}, while the water contact angle decreased from 70.9° to 42.2°, indicating increased hydrophilicity. Blending the grafted CNCs with poly(vinyl alcohol) produced a hydrogen-bonded supramolecular adhesive with a ceramic-lap shear strength of 7.52 MPa; 75% of the initial strength was retained at 100% relative humidity.

Controlled radical polymerization provides greater control over graft architecture. Kedzior *et al.*[52] formed uniform polymer brushes by surface-initiated atom-transfer radical polymerization, allowing graft-chain length and density to be regulated. The modified CNCs showed improved dispersion in organic solvents and stronger compatibility with polymer matrices. Liu *et al.*[53] used reversible addition–fragmentation chain-transfer polymerization to grow functional polymers from CNC surfaces under mild conditions. Adjusting the RAFT-agent-to-monomer ratio controlled graft-layer thickness and functionality, expanding opportunities for responsive materials.

Ring-opening polymerization of ε-caprolactone is another grafting-from route. Chang *et al.*[54] grew poly(ε-caprolactone) chains from CNC hydroxyl sites under catalytic conditions. The modified particles were more compatible with poly(lactic acid), and the grafted PCL provided a plasticizing contribution that increased tensile strength by approximately 90% and elongation at break by about tenfold. The magnitude of this effect depends on graft length, graft density, and the dispersion of modified CNCs in the matrix.

In grafting onto, the polymer is synthesized and characterized before attachment. Shang *et al.*[55] prepared a monofunctional polyurethane prepolymer by controlling the isocyanate-to-polyol ratio and then coupled it to CNC hydroxyl groups. This approach permits the polymer molecular weight and architecture to be established before grafting. Its main limitation is steric hindrance: bulky chains cannot readily reach every surface site, so the attainable graft density is usually lower than in grafting-from processes.

The two polymer-grafting strategies therefore differ in grafting density, control over chain architecture, reaction efficiency, purification requirements, and possible side reactions, as summarized in Table 2. Grafting onto offers prior characterization of the polymer, but is limited by steric hindrance, whereas grafting from generally provides denser surface coverage but requires tighter control of initiation and polymerization.

Table 2
Comparison of "grafting onto" and "grafting from" polymer-grafting strategies

Aspect	"Grafting onto" strategy	"Grafting from" strategy
Basic principle	Pre-synthesized functional polymers are coupled to reactive groups on the CNC surface.	Initiators or catalytic/active sites are first immobilized on CNCs, followed by in situ polymerization from the surface.
Grafting density	Usually relatively low because bulky polymer chains encounter steric hindrance near the CNC surface.	Generally higher because small monomers can more easily diffuse to surface-anchored active sites.
Chain-length controllability	Polymer molecular weight and structure can be characterized before grafting, allowing relatively precise control over chain architecture.	Chain length can be regulated by polymerization conditions, but direct characterization of grafted chains is more difficult unless the chains are cleaved from the surface.
Reaction efficiency	Coupling efficiency may be limited by steric hindrance and incomplete reaction between polymer end groups and CNC surface groups.	Often more efficient for constructing dense polymer layers, especially when controlled/living polymerization is used.
Possible side reaction	Unreacted free polymers may remain in the system and require thorough purification.	Free homopolymer formation, initiator instability, catalyst residues, or uncontrolled polymerization may occur.
Main advantages	Polymer structure and functionality are more predictable; suitable for	Enables high grafting density, tunable surface coverage, and construction of

	introducing well-defined end-functional polymers.	polymer-brush-like CNCs.
Main limitations	Limited grafting density and reduced accessibility of surface reaction sites.	More complex reaction system and more difficult characterization of grafted polymer chains.
Suitable applications	Surface compatibilization, introduction of specific functional polymers, and systems requiring well-defined polymer structures.	High-density surface modification, nanocomposite reinforcement, responsive materials, and polymer-brush construction.

Cationic modification

Cationization introduces permanent positive charge, usually through quaternary-ammonium groups, and can reverse the native negative charge of sulfated or carboxylated CNCs. Covalent grafting or non-covalent adsorption can thereby confer antibacterial activity, affinity for anionic species, and stronger interactions with negatively charged matrices. Charge reversal is useful, but it also changes colloidal stability and compatibility with other formulation components.

Lekjinda *et al.*[56] functionalized cellulose-I/II CNCs with quaternized chitosan, producing positively charged particles with enhanced antibacterial activity and thermal stability. Shi *et al.*[43] classified cationization into epoxy-quaternary-ammonium grafting and cationic-polymer modification. Epoxy reagents such as 2,3-epoxypropyltrimethylammonium chloride can react with CNC hydroxyl groups under alkaline conditions, whereas cationic polymers may be adsorbed electrostatically or coupled covalently. Li *et al.*[57] showed that cationic CNCs interacted strongly with anionic carboxymethyl cellulose, improving dispersion, interfacial bonding, and film strength as the degree of substitution increased. Electrostatic attraction has likewise been used to stabilize cationic waterborne-polyurethane/CNC emulsions and enhance nanocomposite mechanical performance.[58]

Cationization can therefore improve CNC-based antibacterial materials, reinforced composites, and adsorption or interfacial systems. Covalent and non-covalent routes differ in stability, control of substitution, purification requirements, and industrial feasibility; the choice should be matched to the intended medium and application.

Supramolecular engineering strategies

Permanent covalent modification provides durable functionality, but irreversibility is not always desirable. Supramolecular engineering uses hydrogen bonding, electrostatic attraction, metal coordination, hydrophobic association, and host–guest recognition to construct reversible CNC networks. These interactions can reorganize under stress or environmental stimuli, enabling responsive and self-healing behaviour, although the same reversibility also makes the systems sensitive to pH, ionic strength, solvent composition, and temperature.

Hydrogen bond regulation

Hydrogen bonding is the principal non-covalent interaction in CNC self-assembly and gelation. Surface hydroxyl groups act as both donors and acceptors, allowing dynamic interparticle connections and ordered structures to develop. Hydrogen bonds influence not only macroscopic network formation and mechanical response, but also the interaction potential between particles. Duan *et al.*[1] showed that changes in the strength and distribution of hydrogen bonding can regulate the pitch of chiral nematic CNC structures and thereby tune structural colour. Hydrogen bonding is consequently important for maintaining long-range order in CNC photonic assemblies.

In gels, hydrogen bonding contributes to the formation and maintenance of three-dimensional CNC networks. De France *et al.*[59] noted that when electrostatic repulsion is weakened by pH or ionic-strength changes, hydrogen bonding and van der Waals attraction can become dominant and drive a sol–gel transition. Dynamic reconfiguration of these bonds can also dissipate energy. Liang *et al.*[60] constructed a multiple-hydrogen-bond network in which the hydrogel reached an elongation at break above 1450% while retaining conductivity. Hydrogen bonds therefore provide both structural connectivity and a reversible energy-dissipation mechanism.

In complex solvents, hydrogen-bond networks may be transferred or reorganized rather than simply strengthened or weakened. Competition between ionic-liquid components and CNC surface hydroxyl groups can alter both microstructure and macroscopic behaviour. Wang[23] reported that ionic-liquid-induced reorganization increased conductivity and produced highly flexible

materials with elongations at break up to 2400%. Shi *et al.*[43] further described reversible formation and disruption of CNC–poly(ethylene glycol) hydrogen bonds in different solvents, enabling shape-memory and stimulus-responsive behaviour.

Electrostatic interactions

Sulfate and carboxylate groups on CNCs can interact electrostatically with cationic polyelectrolytes, surfactants, or nanoparticles. Coulombic attraction drives directional association at interfaces and can create reversible networks without covalently modifying every component. Because charge density and screening depend on pH and ionic strength, electrostatic assemblies can reorganize and display stimulus response or self-healing, but they may also be destabilized by salts or competing ions.

Qi *et al.*[10] assembled negatively charged CNCs with quaternary-ammonium lignin by adjusting pH, producing a compact layer at the oil–water interface that inhibited Pickering-emulsion coalescence. Changes in pH altered the charge state of the lignin and therefore the assembled structure. Duan *et al.*[1] used cationic polyacrylamide to screen the CNC surface charge; weakened electrostatic repulsion shifted the system from long-range chiral nematic order toward a more disordered structure and produced angle-independent colour. Capron and Cathala[61] emphasized that CNC stability in water arises from surface charge and the electrical double layer. Increasing ionic strength compresses this layer, reduces repulsion, and allows van der Waals attraction to promote aggregation or network formation.

Precise control of the surface charge enables a more ordered molecular assembly. TEMPO-mediated oxidation can create relatively uniform carboxylate sites on CNC surfaces, and the degree of carboxylation can regulate the nanoscale spacing of immobilized molecules, including DNA probes, thereby improving biosensor organization and performance.[43]

Metal coordination

Carboxylated CNCs can coordinate metal ions through lone pairs on carboxylate oxygen atoms. This interaction provides a basis for metal-ion capture, catalytic-site immobilization, and ion-mediated crosslinking. Coordination can strengthen networks, but excessive metal-ion loading can also screen surface charge and promote uncontrolled aggregation.

Multidentate ligands increase the number and strength of coordination sites. Diethylenetriaminepentaacetic dianhydride, for example, can be esterified onto CNC hydroxyl groups to introduce dense polycarboxylate chelating sites; metal loading has been adjusted within 0.213–0.325 wt% by controlling surface functionalization.[43] Tang *et al.*[62] reported that carboxylated CNC materials adsorbed Pb^{2+}, Cd^{2+}, Cu^{2+}, and Cr(VI) through a combination of coordination, electrostatic attraction, and ion exchange. Surface $–COO^-$ groups played a dominant role, and the reported Cd^{2+} removal reached 86.3%.

Hydrophobic interactions

Hydrophobic interactions are important for controlling CNC behaviour at two-phase interfaces. Alkyl, ester, or polymer segments introduced by surface modification reduce surface free energy and promote adsorption at the oil–water interface. The resulting amphiphilic particles can reorganize into dense interfacial films and stabilize Pickering emulsions. Sun *et al.*[17] used a CNC/graphene-oxide composite to stabilize emulsions. The addition of NaCl screened electrostatic repulsion, promoted graphene-oxide enrichment at the interface, and reduced the average droplet diameter from 15.4 to 5.1 μm, demonstrating the coupled roles of wettability and electrostatic interactions.

Kalashnikova *et al.*[63] showed that alkylation increased the CNC contact angle and favoured the formation of dense interfacial particle layers that resisted droplet coalescence. Chain length and degree of substitution were therefore key determinants of adsorption energy and emulsion stability. Capron and Cathala[61] similarly introduced fatty-acid segments by esterification and found that increasing hydrophobic substitution strengthened adsorption at the oil–water interface and reduced sensitivity to changes in ionic strength.

Efficient CNC assembly at oil–water interfaces therefore requires an appropriate balance among hydrophobicity, electrostatic forces, and steric stabilization. The type, chain length, and substitution level of hydrophobic segments determine whether particles can reach the interface, adopt the required wettability, and form a persistent protective layer.

Host-guest interactions

Host–guest interactions arise when guest molecules are selectively included within host cavities, such as the hydrophobic interior of cyclodextrins. Hydrophobic association and size complementarity provide molecular recognition and can enable controlled loading and release. Akhondi *et al.*[64] grafted β-cyclodextrin onto pistachio-shell-derived CNCs through epichlorohydrin crosslinking and used the material to encapsulate propolis extract. The β-cyclodextrin cavities increased the loading of hydrophobic bioactive compounds, and the half-maximal inhibitory concentration against HepG2 cells decreased to 8.122 μg mL^{-1} relative to free propolis. The result illustrates how host–guest chemistry can improve the apparent bioavailability of hydrophobic cargos.

Dynamic covalent bond-mediated adaptive networks

Dynamic covalent bonds provide a complementary route to adaptive CNC networks. Unlike permanent covalent crosslinks, boronate esters, imines, Schiff bases, and related bonds can reversibly associate, dissociate, or exchange under defined conditions. Such chemistry can give CNC hydrogels, coatings, and nanocomposites self-healing, injectability, stress relaxation, and reprocessability. Tang *et al.*[65] used aldehyde-functionalized CNCs and dynamic Schiff-base bonds to construct self-healing, stimulus-responsive hydrogels. Cheng *et al.*[66] combined boronate-ester and acylhydrazone bonds in a highly stretchable, rapidly self-healing nanocellulose hydrogel. Dynamic covalent networks are generally stronger than purely non-covalent assemblies, but their reversibility depends on pH, water content, oxidation degree, crosslinker concentration, and the timescale of the intended function.

Surface molecular engineering and functional material construction

Figure 8 summarizes how the periodic distribution of hydroxyl groups on CNC crystal surfaces can be used for molecular engineering. Controlling the type, density, and spatial distribution of functional groups enables ordered placement of molecular units, regulation of steric effects, and systematic tuning of material structure and performance.[43]

CNCs can act as rigid nanotemplates for spatial control. Selective oxidation or mild derivatization creates regularly distributed reactive sites that can anchor fluorescent molecules at controlled separations. Nanoscale spacing reduces aggregation-induced self-quenching and can therefore support bio-based solid-state luminescent materials with improved emission retention.

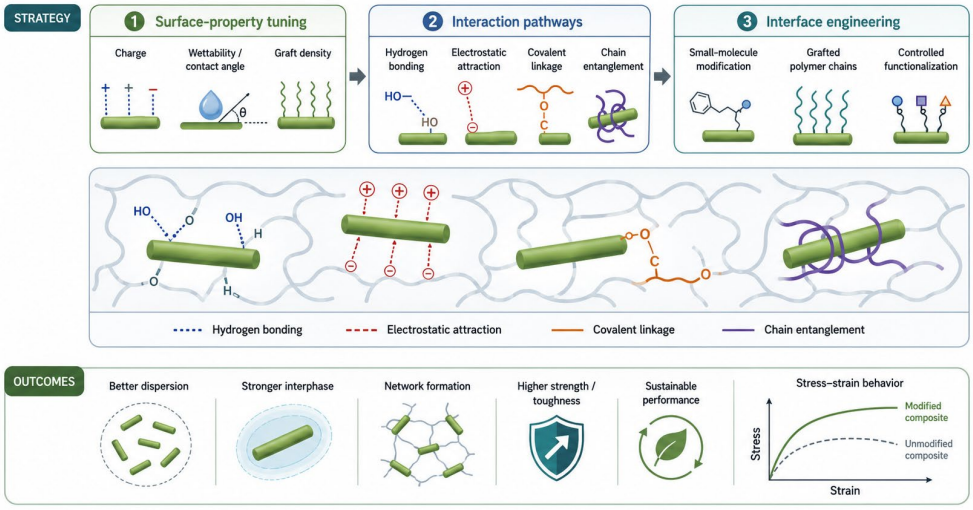


Figure 8: Molecular-interaction and surface-engineering strategies for modified CNC materials, synthesized from Refs. 43,50,52–55,57

Combining multiple surface groups and interactions provides a general route to multifunctionality. Hydrazide-functionalized CNCs can be produced by TEMPO-mediated carboxylation followed by amidation. Reaction with aldehyde-terminated poly(ethylene glycol)

then forms dynamic Schiff-base crosslinks between rigid CNC nanoparticles and flexible polymer segments, generating a three-dimensional aerogel network.

Residual CNC hydroxyl groups and PEG chains can additionally form a dynamic hydrogen-bond network. Changes in solvent polarity reorganize this secondary network and can produce stimulus response, shape-memory behaviour, and reversible shape recovery. The combination of rigid–flexible coupling with multiple reversible interactions is therefore more effective than relying on a single crosslinking mechanism.

APPLICATION AREAS OF CNCs

The high stiffness, surface reactivity, self-assembly and networking capabilities of CNCs have been applied to composite materials, photonic films, sensors, biomedical systems, environmental materials, lubricants and food-related products.

Polymer composites and reinforcement

Biodegradable polymers, coatings, and packaging materials must often gain strength, dimensional stability, and barrier performance without losing processability or sustainability. CNCs provide high crystallinity, large aspect ratio, and high axial stiffness, allowing them to act as nanoscale reinforcing phases. When well dispersed, they form hydrogen-bonded or percolating networks that transfer stress, restrict polymer-chain mobility, and increase the tortuosity of gas-diffusion pathways. Poor dispersion or excessive loading, however, converts this reinforcing network into agglomerated defects.

Lei *et al.*[67] incorporated office-waste-paper-derived CNCs into poly(lactic acid). At 1 wt% CNC, tensile strength increased from 43.44 to 93.54 MPa and elongation at break from 1.8% to 2.9%. These changes indicate that CNCs are not inert fillers: their crystallinity and surface hydroxyl groups promote interfacial interaction and stress transfer. El-Hadi[68] likewise reported that CNCs can contribute to improved mechanical performance in plasticized PLLA/PHB blends, although the response depends on the combined effects of blend composition and plasticizer. In all such systems, the central challenge is to translate nanoscale stiffness into macroscopic properties by controlling surface chemistry, dispersion, and network formation rather than simply increasing filler content.

Photonic structures and optical devices

The principal challenge in CNC photonics is to translate nanoscale chiral order into stable, tunable, and scalable optical responses. Unlike photonic materials that depend on lithography or inorganic building blocks, CNCs spontaneously form chiral nematic structures during evaporation-induced self-assembly. Selective Bragg reflection then produces structural colour, with the reflected wavelength governed mainly by the helical pitch and refractive-index contrast.

The helical pitch is highly sensitive to aspect ratio, surface charge, ionic strength, additives, and drying conditions. Zhang *et al.*[69] showed that ultrasonication changed the pitch from 483 to 501 nm and thereby tuned the structural colour. Sun *et al.*[3] prepared humidity-responsive films from waste-cotton-derived CNCs with different aspect ratios. Moisture uptake expanded the chiral structure and red-shifted the reflection peak, converting humidity into a visible signal without a separate electronic readout. Such behaviour is promising for intelligent packaging, humidity sensing, and anti-counterfeiting, although large-area colour uniformity and batch reproducibility remain practical limitations.

CNCs can also serve as chiral templates for more complex optical functions. Zhao *et al.*[70] incorporated carbon quantum dots into a CNC chiral matrix to combine structural colour with ultraviolet-excited fluorescence. Cao *et al.*[71] used CNC chiral nematic order to induce circularly polarized emission from lignosulfonate, producing a bio-based film with circularly polarized luminescence and room-temperature phosphorescence. CNC-based structural-colour composite films have additionally been investigated for passive radiative cooling, broadening the role of photonic order from visual appearance to thermal management.[72] These examples show that a renewable self-assembled chiral platform can integrate reflection, fluorescence, phosphorescence, and information-encoding functions.

Sensing and wearable devices

Flexible sensors and smart windows require a balance among optical response, conductivity, mechanical durability, and environmental stability. CNCs contribute through several complementary mechanisms: their rod-like morphology and surface hydroxyl groups reinforce polymer networks through hydrogen bonding; charged surfaces support ion transport and interfacial

coupling; and chiral nematic self-assembly converts deformation or environmental changes into visible colour shifts. CNCs can therefore function as reinforcing nanofillers, colloidal stabilizers, photonic building blocks, and interfacial modifiers within the same device.

Thermoresponsive optical devices must regulate solar transmission while retaining optical uniformity and colloidal stability. Shi and Zhou[73] incorporated hollow polydopamine and CNCs into poly(N-isopropylacrylamide) microgels for thermochromic smart windows. PNIPAm supplied the volume-phase transition, hollow polydopamine enhanced solar absorption and photothermal conversion, and CNCs stabilized the microgel dispersion. At 0.3 wt% hollow polydopamine, the solar-modulation efficiency reached 37.0% and the maximum indoor–outdoor temperature difference was 45.8 °C. CNCs therefore improved performance mainly by maintaining a uniform responsive microstructure.

Wearable sensors must withstand large deformation while maintaining mechanical strength and reliable electrical output. CNCs can provide dynamic hydrogen-bonded crosslinks that dissipate energy and stabilize conductive pathways. Liang *et al.*[60] prepared a CNC/polyacrylamide–sodium-hyaluronate semi-interpenetrating hydrogel in which CNCs acted as reinforcing domains and reversible crosslinking sites. The elongation at break exceeded 1450% and ionic conductivity reached 5.22×10^{-2} S m^{-1}. Alghamdi *et al.*[74] combined CNCs with graphene in a triboelectric nanogenerator for harvesting mechanical energy from daily activity. The reported power density was 0.4 W cm^{-2} and output stability was maintained for up to 3 years, indicating a possible contribution of CNCs to long-term structural integrity.

Stimulus-responsive photonic hydrogels and fibres provide a direct route to visual sensing because swelling, stretching, or compression changes the chiral pitch and shifts the reflected wavelength. Wang *et al.*[75] prepared iridescent hydrogel fibres from ascidian-derived CNCs, sodium alginate, and acrylamide through pre-gelation, nanostructure orientation, ion chelation, and solvent exchange in a glycerol–water medium. The fibres had a tensile strength of 1.38 MPa, responded continuously over 11–98% relative humidity with a maximum 170 nm blue shift, and exhibited wavelength shifts of up to 80 nm during cyclic strains below 50%. These results demonstrate visual monitoring of complex deformation and humidity.

Coupling a CNC photonic structure with a conductive network enables simultaneous optical and electrical sensing. Yu *et al.*[76] prepared a cellulose-nanofibre mechanochromic hydrogel by gas-phase acid curing after TEMPO-mediated oxidation. A load as low as 0.36 N produced a visible colour change corresponding to 1.2 kPa stress and 15% strain. Lu *et al.*[77] developed a force-responsive sandwich hydrogel in which a photonic-crystal core was separated from conductive outer layers. Interpenetration and entanglement of PVA chains strengthened the interfaces. The material showed continuous red-to-blue colour changes and synchronous resistance changes at tensile strains up to 130% and compressive strains up to 49%, allowing finger-motion and speech-related signals to be detected.

Sweat-responsive patches move CNC sensing closer to wearable use because they must combine physiological monitoring with flexibility, breathability, and biocompatibility. Qian *et al.*[78] incorporated phytic acid into a CNC/PVA photonic patch. Phytic acid strengthened hydrogen bonding and produced a toughness of 1.4 MJ m^{-3} and conductivity of 10 mS cm^{-1}. Contact with sweat changed the colour progressively from blue to red through green and yellow states while generating selective ion-sensitive electrical signals. The design illustrates how CNC networks can integrate colourimetric feedback, ion conduction, mechanical deformation, and real-time monitoring.

Biomedical and food-related applications

Biomedical materials and food packaging often rely on synthetic polymers, inorganic fillers, or separate indicators, which can limit degradability, biocompatibility, responsiveness, or interfacial stability. CNCs provide renewable and potentially biodegradable scaffolds with hydroxyl or carboxyl groups capable of hydrogen bonding, electrostatic interaction, Schiff-base formation, supramolecular assembly, and chiral nematic self-assembly. They can therefore serve as reinforcing fillers, carriers for bioactive molecules, interfacial stabilizers, dynamic crosslinking sites, photonic scaffolds, and barrier-enhancing components.

Hemostatic and wound-dressing materials must combine rapid coagulation, fluid absorption, biocompatibility, antibacterial activity, and integrity under wet physiological conditions. Yadav *et al.*[79] freeze-dried microfibrillated

cellulose, carboxylated CNCs, and cinnamon extract into a microporous sponge. The porous skeleton promoted fluid uptake, while carboxylated CNCs strengthened the network and supplied negatively charged sites. In a mouse liver-injury model, the sponge reached a swelling ratio of 1435%, an in vitro coagulation index of approximately 40%, a hemostasis time of 45 s, and about 50% less blood loss than medical gauze. Liu *et al.*[80] incorporated tunicate CNCs into supramolecular hydrogels through Schiff-base and hydrogen-bond interactions. The reversible network improved antibacterial, hemostatic, and mechanical performance, demonstrating that CNCs can reinforce dressings while regulating dynamic biological interfaces.

Drug-delivery systems require high loading, controlled release, biocompatibility, and response to physiological conditions. Sharifabad *et al.*[81] designed a glucose-responsive insulin nanocarrier based on CNC cores, poly(propylene imine) dendrimers, and 4-carboxyphenylboronic acid. The dendritic layer increased drug-binding sites and phenylboronic acid supplied reversible glucose recognition. Encapsulation efficiency reached 85.8%, drug loading 21.7%, and insulin release 65% under high-glucose conditions, compared with 10% in simulated gastric fluid at pH 1.2. Li *et al.*[82] prepared holocellulose nanocrystals from burdock insoluble dietary fibre; hydrophobic interactions and hydrogen bonding with digestive enzymes delayed starch hydrolysis in a dose- and particle-size-dependent manner. Shafique *et al.*[83] used an alginate/CNC matrix to support a photodynamic metal–organic framework that generated reactive oxygen species and inhibited *Escherichia coli*, *Staphylococcus aureus*, and *Bacillus subtilis*. For blood-contact applications, Zhao *et al.*[84] used shear-aligned CNCs to organize zwitterionic hydrogel coatings inspired by vascular endothelium. The resulting hydration layer reduced nonspecific protein adsorption and thrombosis, while adhesion to PVC exceeded 800 J m^{-2} and remained stable under shear, abrasion, and water washing.

Flexible bioelectronics and electronic skin require stretchability, conductivity, self-healing, and reliable strain response. CNCs can act as reinforcing domains, hydrogen-bonding crosslinkers, and regulators of pore and ion-transport structure. Ullah *et al.*[85] constructed a CNC-reinforced conductive hydrogel through hydrophobic association. Hydrogen bonding between CNC hydroxyl groups and the acrylamide/butyl-acrylate network increased strength and energy dissipation. The hydrogel reached a tensile strength of 371.2 kPa, fracture strain of 2108%, conductivity of 420 mS m^{-1}, and response time of 140 ms. After self-healing, it still sustained 499% strain and 197 kPa stress, showing that reversible CNC-mediated interactions can support network reconstruction.

In food systems, the high aspect ratio and hydroxyl-rich surface of CNCs increase the tortuosity of gas-diffusion paths and can improve mechanical and barrier properties, while chiral nematic assembly produces visible stimulus-responsive colour. Mu *et al.*[86] reviewed CNCs as reinforcing and barrier fillers for biodegradable packaging; modified CNCs in PLA films reduced oxygen transmission by 34% through a combination of tortuous paths and improved interfacial compatibility. Yan *et al.*[87] described chiral CNC films responsive to humidity, pH, and volatile gases. CNC/anthocyanin labels use the CNC matrix as a renewable film-forming scaffold and anthocyanins as pH-responsive chromophores for monitoring meat and seafood spoilage. CNC/silver-nanoparticle composites can respond to H_2S, while CNC-stabilized Pickering emulsions can encapsulate essential oils for sustained antimicrobial release. CNC packaging can therefore integrate barrier protection, visual freshness indication, antimicrobial activity, and controlled release within a biodegradable platform.

Environmental applications

Environmental remediation requires low-density, renewable, efficient, and reusable materials for oil–water separation, toxic-ion adsorption, pollutant degradation, and selective transport. CNCs offer high specific surface area, hydroxyl and carboxyl functionalities, adjustable wettability, and network-forming ability, allowing them to act as structural frameworks, adsorption sites, interfacial modifiers, and functional carriers. He *et al.*[88] prepared CNC-derived carbon aerogels with radially aligned channels by directional freeze-drying and carbonization. After polydimethylsiloxane modification, the aerogels had a water contact angle of 135°, oil–water separation efficiencies of 98.2–99.5%, and fluxes up to 14,023 L m^{-2} h^{-1}. Radial pores reduced flow resistance, hydrophobic modification improved selectivity, and solar heating reduced oil viscosity and shortened absorption time by 41.7%. Ren *et al.*[89] reported cellulose-based hydrophobic carbon aerogels with oil/solvent capacities of 12.7–49.8 g

g^{-1} and partial capacity retention after repeated compression, demonstrating potential for reusable treatment of oily food-processing wastewater.

For heavy-metal and organic-pollutant removal, CNC hydroxyl and carboxyl groups provide sites for electrostatic attraction, hydrogen bonding, and coordination, while porous networks expose these sites and improve mass transfer. Cheng *et al.*[90] prepared CNC/PVA aerogels for Cr(VI) adsorption. Directional lamellae supplied accessible adsorption surfaces and diffusion pathways, while CNCs reinforced the aerogel framework. CNC hydrogels can also immobilize enzymes for active pollutant degradation. Shu and Yan[91] immobilized laccase within a CNC-containing hydrogel network for degradation of phenolic compounds. The hydrated porous matrix supported enzyme stability and substrate transport, extending the CNC role from passive adsorption to a reusable catalytic platform.

Water-treatment and ion-transport membranes must combine scalable manufacture, separation efficiency, and controlled transport pathways. CNCs can reinforce membranes, regulate pore structure, and provide hydrophilic channels for water or ions. Ding *et al.*[92] prepared CNC/PVA membranes from waste-paper pulp by evaporation-induced self-assembly and glutaraldehyde crosslinking. The estimated production cost was US$2.45 m^{-2}, no organic solvent was used, and energy consumption was reduced by 45% relative to conventional ultrafiltration membranes. Liu *et al.*[93] incorporated CNCs into sulfonated poly(ether ether ketone) membranes for vanadium redox-flow batteries, obtaining a proton conductivity of 0.073 S cm^{-1} and a voltage efficiency of 88.7%. Hydrophilic CNC interfaces promoted continuous proton-transport pathways, while helping to retain dimensional stability, illustrating applications beyond conventional pollutant filtration.

Tribology and wear-resistant systems

Tribological materials must provide friction reduction, wear resistance, dispersion stability, environmental compatibility, and long service life. Conventional additives often rely on inorganic nanoparticles or persistent synthetic compounds that may sediment or create environmental concerns. CNCs offer a renewable alternative: their nanorod morphology allows entry into contact zones, and polar surface groups promote adsorption on rubbing surfaces. During sliding, deposited CNCs can fill surface defects, smooth asperities, assist heat dissipation, and form protective boundary layers. These benefits depend, however, on stable dispersion and effective transport of the particles into the contact interface.

In liquid lubrication, CNC performance is associated with interfacial adsorption and surface repair. Guimarey *et al.*[94] dispersed CNCs in isopropyl palmitate to form a stable bio-based nanolubricant. Rod-like particles entered the contact region and adsorbed through their polar hydroxyl groups, reducing the coefficient of friction by 44% and improving wear resistance. Filling of microdefects and formation of a more uniform boundary layer contributed to the response, while improved thermal conductivity assisted frictional-heat dissipation.

For water-based lubrication, stable dispersion and persistent lubricating film formation are the principal challenges. Zhang *et al.*[95] compared sulfated and carboxylated CNC additives at concentrations below 1 wt%. Sulfated CNCs formed liquid-crystalline structures above 0.5 wt%, and at 0.5 wt% they reduced the coefficient of friction by 63.4%. Strongly dissociated sulfate half-esters provide long-range electrostatic repulsion that favours chiral or shear-induced ordering; under sliding, aligned domains can form compact boundary films, reduce direct asperity contact, and distribute load. Carboxylated CNCs also carry negative charge, but carboxyl-group ionization is more sensitive to pH, ionic strength, and counterion screening. Oxidation may additionally alter aspect ratio, charge distribution, and hydration. Carboxylated CNCs can still reduce friction through adsorption, defect filling, and polishing, but may be less able to maintain the ordered, shear-aligned films observed for sulfated CNCs. Lubrication therefore depends on surface-group chemistry and ionization as well as particle morphology.

Partial carbonization can further alter the lubrication mechanism. Cheng *et al.*[96] used ionic-liquid-assisted heat treatment to produce hybrid particles containing rod-like CNC residues and low-crystallinity carbon regions. As water-based lubricant additives, these particles reduced the coefficient of friction by 39.1% and wear volume by 76.8% while retaining good dispersion stability. Synergistic adsorption of residual cellulose structures and carbonaceous domains formed a network-like interfacial film that combined aqueous dispersibility with load-bearing and lubricating functions.

In polymer coatings, CNCs act as stiff, high-surface-area reinforcing fillers whose hydroxyl

groups interact with the matrix. Samyn and Cosemans[97] compared microcrystalline cellulose, CNCs, cellulose nanofibres, cellulose microfibres, and hydrophobically modified microfibres in waterborne epoxy coatings. At 0.75 wt% CNC, coating hardness increased by 32%, elastic modulus by 20%, glass-transition temperature by 1.6 °C, and wear resistance by 33% relative to neat epoxy. These changes were attributed to a continuous nanofiller network that improved load transfer and restricted polymer-chain motion. Cellulose nanofibres produced a larger 58% reduction in wear at the same loading, consistent with their higher aspect ratio and specific surface area. The comparison highlights morphology-controlled network formation as a determinant of coating performance.

OUTLOOK AND FUTURE CHALLENGES

CNC research now extends well beyond the isolation of crystalline nanoparticles. Surface chemistry can be tailored, self-assembly can be directed, and multifunctional material systems can be constructed around the particles. The remaining challenges are closely interconnected: batch-to-batch reproducibility, whole-process environmental performance, long-term durability, safety, standardization, and genuinely scalable production.

Scale-up must be evaluated across the complete process rather than by considering a single reagent or unit operation. Eliminating mineral acid is advantageous only when the alternative does not impose excessive electricity consumption, long residence times, difficult solvent purification, or low solids throughput. ILs and DESs can be recovered at rates above 90%, but solvent price, viscosity, water sensitivity, and cumulative losses remain important. Enzymatic and bacterial routes use mild conditions, but generally have slower kinetics and lower productivity. Future studies should therefore report mass and energy balances alongside yield, crystallinity, and particle dimensions. Continuous operation, higher solids loading, closed-loop solvent recovery, and pretreatments that reduce mechanical energy deserve priority; even a 95% recovery rate represents a 5% loss per cycle unless that loss is controlled.

A second priority is the control and characterization of surface heterogeneity. A single average degree of substitution does not reveal whether functional groups are uniformly distributed, concentrated at defects, or confined to particular crystal faces. Such differences affect colloidal stability, graft accessibility, self-assembly, and interfacial load transfer. Controlled radical polymerization, click chemistry, and selective oxidation are useful only when group density and spatial distribution can be quantified. Combining spectroscopy, scattering, microscopy, titration, and molecular simulation should make structure–property relationships more predictive.

Application studies must also move beyond short-term peak performance. Composite formulations must retain dispersion during realistic processing; photonic films require uniform colour over large areas; sensors must distinguish target signals from humidity, temperature, and mechanical drift; and biomedical systems require dose-dependent toxicology, degradation studies, and *in vivo* evidence. Standardized controls and durability tests under relevant service conditions would make comparisons among studies more meaningful. Peak values are easy to report, whereas stability and reliability require longer-term evidence.

Translation is further limited by inconsistent material definitions. CNC batches are often identified only by source or preparation route even though particle-size distribution, crystallinity, sulfate or carboxyl content, counterions, residual impurities, and moisture history may differ substantially. Minimum reporting standards, reference methods, and interlaboratory testing would improve reproducibility. Ecotoxicity, occupational exposure, and end-of-life behaviour should be evaluated during material development rather than after a formulation has been fixed. A material name alone is not a material specification.

The most credible path forward is to design the isolation route and surface chemistry for a defined function, test the material under realistic conditions, and quantify cost and environmental burden across the life cycle. This approach would distinguish applications in which CNCs provide a genuine system-level advantage from those in which they merely replace another nanoscale additive. Shared characterization standards and closer collaboration among process engineers, chemists, materials scientists, toxicologists, and manufacturers will be necessary to move CNCs from versatile laboratory building blocks to reliable components of sustainable material systems.

REFERENCES

[1] C. L. Duan, Thesis, South China University of Technology, Guangzhou, 2024, https://doi.org/10.27151/d.cnki.ghnlu.2024.000353

[2] H. Hu, Thesis, Tianjin University of Science and Technology, Tianjin, 2024, https://doi.org/10.27359/d.cnki.gtqgu.2024.001031

[3] J. Sun, J. Tan, T. Tian, C. Zhang and C. Wang, *Int. J. Biol. Macromol.*, **319**, 145473 (2025), https://doi.org/10.1016/j.ijbiomac.2025.145473

[4] Y. Zhao, Y. Zhang, M. E. Lindström and J. Li, *Carbohyd. Polym.*, **117**, 286 (2015), https://doi.org/10.1016/j.carbpol.2014.09.020

[5] R. W. Ren, X. Q. Chen and W. H. Shen, *Int. J. Biol. Macromol.*, **202**, 1 (2022), https://doi.org/10.1016/j.ijbiomac.2022.01.009

[6] X. Tong, W. Shen, X. Chen, M. Jia and J.-P. Corriou, *J. Appl. Polym. Sci.*, **137**, 48407 (2020), https://doi.org/10.1002/app.48407

[7] E. Lam and U. D. Hemraz, *Nanomaterials*, **11**, 1641 (2021), https://doi.org/10.3390/nano11071641

[8] T. F. Meyabadi, F. Dadashian, G. M. M. Sadeghi and H. E. Zanjani Asl, *Powder Technol.*, **261**, 232 (2014), https://doi.org/10.1016/j.powtec.2014.04.039

[9] N. Flores-Ramírez, A. N. Yhamel-García, S. R. Vásquez-García, H. Martínez Flores, L. Domratcheva-Lvova *et al.*, *Cellulose Chem. Technol.*, **52**, 35 (2018), https://www.cellulosechemtechnol.ro/pdf/CCT1-2(2018)/p.35-41.pdf

[10] J. L. Qi, Thesis, Tianjin University of Science and Technology, Tianjin, 2024, https://doi.org/10.27359/d.cnki.gtqgu.2024.001114

[11] X. Y. Tan, S. B. Abd Hamid and C. W. Lai, *Biomass Bioenerg.*, **81**, 584 (2015), https://doi.org/10.1016/j.biombioe.2015.08.016

[12] L. Güemes, V. Calvo, V. B. Maya-Segura, E. Pires, W. K. Maser *et al.*, *Carbohyd. Polym. Technol. Appl.*, **13**, 101080 (2026), https://doi.org/10.1016/j.carpta.2025.101080

[13] B. Fan, L. Zhou, L. Xing and W. Zhang, *Food Hydrocoll.*, **166**, 111355 (2025), https://doi.org/10.1016/j.foodhyd.2025.111355

[14] M. Z. Birhanu, M. G. Tadesse, R. K. Bachheti, I. N. Ahmed and A. Bachheti, *Int. J. Biol. Macromol.*, **335**, 149007 (2026), https://doi.org/10.1016/j.ijbiomac.2025.149007

[15] J. Xu, L. Lin, X. Liang, W. Zha, W. Yin *et al.*, *Food Hydrocoll.*, **167**, 111385 (2025), https://doi.org/10.1016/j.foodhyd.2025.111385

[16] C. Fraschini, G. Chauve and J. Bouchard, *Cellulose*, **24**, 2775 (2017), https://doi.org/10.1007/s10570-017-1319-5

[17] W. Sun, Z. Zhang, Z. Zhang, N. He, Q. Wei *et al.*, *Sci. China Mater.*, **67**, 3225 (2024), https://doi.org/10.1007/s40843-024-3040-5

[18] Y. Yan, M. Zu, Y. Yi, X. Tian, J. Li *et al.*, *Acta Mater. Compos. Sin.*, **42**, 3082 (2025), https://doi.org/10.13801/j.cnki.fhclxb.20240919.003

[19] N. M. Park, S. Choi, J. E. Oh and D. Y. Hwang, *Carbohyd. Polym.*, **223**, 115114 (2019), https://doi.org/10.1016/j.carbpol.2019.115114

[20] R. Aguado, Q. Tarrés, M. À. Pèlach, P. Mutjé, E. de la Fuente *et al.*, *Nanomaterials*, **12**, 1612 (2022), https://doi.org/10.3390/nano12091612

[21] X. Yang, F. Han, C. Xu, S. Jiang, L. Huang *et al.*, *Ind. Crop. Prod.*, **109**, 241 (2017), https://doi.org/10.1016/j.indcrop.2017.08.032

[22] X. Kang, S. Kuga, C. Wang, Y. Zhao, M. Wu *et al.*, *ACS Sustain. Chem. Eng.*, **6**, 2954 (2018), https://doi.org/10.1021/acssuschemeng.7b02363

[23] X. Wang, Thesis, Qilu University of Technology, Jinan, 2025, https://doi.org/10.27278/d.cnki.gsdqc.2025.000638

[24] Y. Tang, H. Yang and S. Vignolini, *Adv. Sustain. Syst.*, **6**, 2100100 (2022), https://doi.org/10.1002/adsu.202100100

[25] Z. L. Song, Thesis, Wuhan Polytechnic University, Wuhan, 2025, https://doi.org/10.27776/d.cnki.gwhgy.2025.000845

[26] R. M. Cherian, T. Antony, R. T. Varghese, B. Akhila, V. Abhijith *et al.*, *Int. J. Biol. Macromol.*, **305**, 141192 (2025), https://doi.org/10.1016/j.ijbiomac.2025.141192

[27] L. Chen, J. Y. Zhu, C. Baez, P. Kitin and T. Elder, *Green Chem.*, **18**, 3835 (2016), https://doi.org/10.1039/C6GC00687C

[28] Y. Zhou, T. Saito, L. Bergström and A. Isogai, *Biomacromolecules*, **19**, 633 (2018), https://doi.org/10.1021/acs.biomac.7b01730

[29] X. Lin, W. Su and Q. Zhang, *Carbohyd. Polym.*, **368**, 124183 (2025), https://doi.org/10.1016/j.carbpol.2025.124183

[30] Y. A. Zhao, Thesis, Huazhong Agricultural University, Wuhan, 2024, https://doi.org/10.27158/d.cnki.ghznu.2024.001420

[31] M. A. Mariño, D. Rueda-Ordonez, M. G. Paredes, R. A. Tapia, R. Pita *et al.*, *J. Clean. Prod.*, **472**, 143461 (2024), https://doi.org/10.1016/j.jclepro.2024.143461

[32] H. Abushammala, I. Krossing and M.-P. Laborie, *Carbohyd. Polym.*, **134**, 609 (2015), https://doi.org/10.1016/j.carbpol.2015.07.079

[33] G. Nicastro, A. Fahimi, A. Dufresne, E. Vahidi, C. Punta *et al.*, *Carbohyd. Polym.*, **369**, 124310 (2025), https://doi.org/10.1016/j.carbpol.2025.124310

[34] A. Lu, X. Yu, Q. Ji, L. Chen, A. E.-G. Yagoub *et al.*, *Ind. Crop. Prod.*, **195**, 116415 (2023), https://doi.org/10.1016/j.indcrop.2023.116415

[35] Y. Jabalera, D. Dahiya, C. D. O. Cencerrado, A. J. Caballero, N. Zaldua *et al.*, *Carbohyd. Polym.*, **357**, 123469 (2025), https://doi.org/10.1016/j.carbpol.2025.123469

[36] V. S. Soeiro, L. L. Tundisi, L. C. L. Novaes, P. G. Mazzola, N. Aranha *et al.*, *Carbohyd. Polym. Technol. Appl.*, **2**, 100155 (2021), https://doi.org/10.1016/j.carpta.2021.100155

[37] D. K. Arserim-Uçar, F. Korel, L. Liu and K. L. Yam, *Food Chem*., **336**, 127597 (2021), https://doi.org/10.1016/j.foodchem.2020.127597
[38] M. Peña-Ortiz, A. García, S. M. Martirani-Von Abercron, P. Marín, S. Marqués *et al*., *Polymers*, **17**, 1240 (2025), https://doi.org/10.3390/polym17091240
[39] Z. Pang, P. Wang and C. Dong, *Cellulose*, **25**, 7053 (2018), https://doi.org/10.1007/s10570-018-2070-2
[40] D. Z. Haddis, M. Chae, J. Asomaning and D. C. Bressler, *Carbohyd. Polym*., **323**, 121460 (2024), https://doi.org/10.1016/j.carbpol.2023.121460
[41] B. Pereira and V. Arantes, *Ind. Crop. Prod*., **152**, 112377 (2020), https://doi.org/10.1016/j.indcrop.2020.112377
[42] A. Kaboorani and B. Riedl, *Ind. Crop. Prod*., **65**, 45 (2015), https://doi.org/10.1016/j.indcrop.2014.11.027
[43] Z. Shi, S. Li, M. Li, L. Gan and J. Huang, *J. Appl. Polym. Sci*., **138**, 51555 (2021), https://doi.org/10.1002/app.51555
[44] Y. Niu, L. Fu, K. Liu, H. Liu, D. Zhang *et al.*, *Food Hydrocoll*., **174**, 112372 (2026), https://doi.org/10.1016/j.foodhyd.2025.112372
[45] P. Du, Y. Xu, J. Wang, X. Yue, M. Gao *et al.*, *Int. J. Biol. Macromol*., **311**, 143391 (2025), https://doi.org/10.1016/j.ijbiomac.2025.143391
[46] M. Roman and W. T. Winter, *Biomacromolecules*, **5**, 1671 (2004), https://doi.org/10.1021/bm034519+
[47] S. Beck-Candanedo, M. Roman and D. G. Gray, *Biomacromolecules*, **6**, 1048 (2005), https://doi.org/10.1021/bm049300p
[48] Y. Habibi, L. A. Lucia and O. J. Rojas, *Chem. Rev*., **110**, 3479 (2010), https://doi.org/10.1021/cr900339w
[49] L. Gan, J. Liao, N. Lin, C. Hu, H. Wang *et al*., *ACS Omega*, **2**, 4725 (2017), https://doi.org/10.1021/acsomega.7b00532
[50] C. Goussé, H. Chanzy, G. Excoffier, L. Soubeyrand and E. Fleury, *Polymer*, **43**, 2645 (2002), https://doi.org/10.1016/S0032-3861(02)00051-4
[51] L. Zhang, Y. Sun, S. Huang, H. Xu, Z. Zhang *et al.*, *Carbohyd. Polym*., **363**, 123705 (2025), https://doi.org/10.1016/j.carbpol.2025.123705
[52] S. A. Kedzior, M. Kiriakou, E. Niinivaara, M. A. Dubé, C. Fraschini *et al*., *ACS Macro Lett*., **7**, 990 (2018), https://doi.org/10.1021/acsmacrolett.8b00334
[53] T. Liu, E. Ding and F. Xue, *Cellulose*, **25**, 1705 (2018), https://doi.org/10.1007/s10570-018-1685-7
[54] P. R. Chang, F. J. Ai, Y. Chen, A. Dufresne and J. Huang, *J. Appl. Polym. Sci*., **111**, 619 (2009), https://doi.org/10.1002/app.29060
[55] W. Shang, J. Huang, H. Luo, P. R. Chang, J. Feng *et al*., *Cellulose*, **20**, 179 (2013), https://doi.org/10.1007/s10570-012-9795-0
[56] K. Lekjinda, P. Pantamanatsopa, P. Sunintaboon, K. Sungsanit and W. Ariyawiriyanan, *Ind. Crop. Prod*., **238**, 122391 (2025), https://doi.org/10.1016/j.indcrop.2025.122391
[57] M.-C. Li, C. Mei, X. Xu, S. Lee and Q. Wu, *Polymer*, **107**, 200 (2016), https://doi.org/10.1016/j.polymer.2016.11.022
[58] H.-C. Chen, Y.-C. Huang, C.-H. Wu, R.-J. Jeng and F.-C. Chang, *Cellulose*, **30**, 2217 (2023), https://doi.org/10.1007/s10570-022-04989-6
[59] K. J. de France, T. Hoare and E. D. Cranston, *Chem. Mater*., **29**, 4609 (2017), https://doi.org/10.1021/acs.chemmater.7b00531
[60] J. J. Liang, Thesis, Jianghan University, Wuhan, 2025, https://doi.org/10.27800/d.cnki.gjhdx.2025.000237
[61] I. Capron and B. Cathala, *Biomacromolecules*, **14**, 291 (2013), https://doi.org/10.1021/bm301871k
[62] J. Tang, J. Sisler, N. Grishkewich and K. C. Tam, *J. Colloid Interface Sci*., **494**, 397 (2017), https://doi.org/10.1016/j.jcis.2017.01.077
[63] I. Kalashnikova, H. Bizot, B. Cathala and I. Capron, *Biomacromolecules*, **13**, 267 (2012), https://doi.org/10.1021/bm201599j
[64] M. Akhondi, Z. S. Korrani, M. Mohammad-Sadeghipour, R. Bahramabadi and M. Mohamadi, *Sci. Rep*., **15**, 24799 (2025), https://doi.org/10.1038/s41598-025-08622-x
[65] J. Tang, M. U. Javaid, C. Pan, G. Yu, R. M. Berry *et al.*, *Carbohyd. Polym*., **229**, 115486 (2020), https://doi.org/10.1016/j.carbpol.2019.115486
[66] H. Cheng, Z. Fan, Z. Wang, Z. Guo, J. Jiang *et al*., *Int. J. Biol. Macromol*., **245**, 125471 (2023), https://doi.org/10.1016/j.ijbiomac.2023.125471
[67] W. Q. Lei, C. Zhou, J. B. Hu, P. Y. Jia, L. Li *et al*., *Biomass Chem. Eng*., **59**, 54 (2025)
[68] A. M. El-Hadi, *Sci. Rep*., **7**, 46767 (2017), https://doi.org/10.1038/srep46767
[69] Y. Zhang, D. Li, Z. Xiong, C. Wu, M. Li *et al*., *Chem. Res*., **36**, 148 (2025)
[70] X. Zhao, H. Feng, B. Yang, Y. Ma, X. Li *et al*., *J. Lumin*., **264**, 120191 (2023), https://doi.org/10.1016/j.jlumin.2023.120191
[71] M. Cao, Y. Ren, Y. Wu, J. Shen, S. Li *et al*., *Nat. Commun*., **15**, 2375 (2024), https://doi.org/10.1038/s41467-024-45844-5
[72] B. Y. Sun, B. An, W. Y. Sun, C. H. Ma, M. C. Xu *et al*., *Acta Mater. Compos. Sin*., **42**, 2174 (2025), https://doi.org/10.13801/j.cnki.fhclxb.20240718.002
[73] S. Shi and Y. M. Zhou, *J. Mater. Sci. Eng*., **43**, 778 (2025), https://doi.org/10.14136/j.cnki.issn1673-2812.2025.05.010
[74] M. S. Alghamdi, J. J. Morgan, K. Walsh, D. W. Shin, R. Nigmatullin *et al.*, *Nano Energy*, **138**, 110816 (2025), https://doi.org/10.1016/j.nanoen.2025.110816
[75] J. Wang, Z. Zhou, X. Li and C. Chang, *Int. J. Biol. Macromol*., **275**, 133501 (2024), https://doi.org/10.1016/j.ijbiomac.2024.133501
[76] J. Yu, S. Gong, C. Xu, L. Jiang, J. Liu *et al*., *Carbohyd. Polym*., **362**, 123678 (2025), https://doi.org/10.1016/j.carbpol.2025.123678
[77] D. Lu, Z. Fang and Z. Qiao, *Nano Lett*., **25**, 2850 (2025), https://doi.org/10.1021/acs.nanolett.4c06047
[78] Y. Qian, H. Wang, Z. Qu, Q. Li, D. Wang *et al.*, *Mater. Horiz*., **12**, 499 (2025), https://doi.org/10.1039/D4MH01148A

[79] C. Yadav, A. Saini, K. Li, S. Chawla, X. Li *et al*., *Cellulose*, **30**, 5857 (2023), https://doi.org/10.1007/s10570-023-05252-2
[80] X. Liu, Y. Zhang, Y. Liu, S. Hua, F. Meng *et al*., *Int. J. Biol. Macromol*., **240**, 124365 (2023), https://doi.org/10.1016/j.ijbiomac.2023.124365
[81] A. H. Sharifabad, T. Behzad and M. Salami-Kalajahi, *Adv. Sens. Energy Mater*., **5**, 100179 (2026), https://doi.org/10.1016/j.asems.2026.100179
[82] Y. Li, W. Liang, M. Huang, W. Huang and J. Feng, *Food Funct*., **13**, 170 (2022), https://doi.org/10.1039/D1FO02012A
[83] B. Shafique, J. Xu, X. Li, J. Xie and Z. Ding, *Food Packag. Shelf Life*, **52**, 101643 (2025), https://doi.org/10.1016/j.fpsl.2025.101643
[84] Z. Zhao, Y. Meng, M. Yao and Y. Wei, *Adv. Healthc. Mater*., **15**, e05805 (2026), https://doi.org/10.1002/adhm.202505805
[85] R. Ullah, L. A. Shah and M. T. Khan, *Int. J. Biol. Macromol*., **260**, 129376 (2024), https://doi.org/10.1016/j.ijbiomac.2024.129376
[86] R. Mu, X. Hong, Y. Ni, Y. Li, J. Pang *et al*., *Trends Food Sci. Technol*., **93**, 136 (2019), https://doi.org/10.1016/j.tifs.2019.09.013
[87] X. Yan, Z. Li, W. Cheng, R. Chen, J. Liu *et al*., *Trends Food Sci. Technol*., **163**, 105163 (2025), https://doi.org/10.1016/j.tifs.2025.105163
[88] Y. He, M. Li, G. Cavallaro and M. Liu, *Chem. Eng. J*., **526**, 170770 (2025), https://doi.org/10.1016/j.cej.2025.170770
[89] M. Ren, O. A. Fakayode, F. Kong, C. Zhou, L. Chen *et al*., *Ind. Crop. Prod*., **197**, 116653 (2023), https://doi.org/10.1016/j.indcrop.2023.116653
[90] R. R. Cheng, K. W. Zhang and Q. Y. Ye, *Shanghai Chem. Ind*., **49**, 24 (2024)
[91] S. C. Shu and H. T. Yan, *Chem. Reagents*, **48**, 52 (2026), https://doi.org/10.13822/j.cnki.hxsj.2025.0275
[92] A. Ding, Y. Wang, Z. Liu, S. Li, H. Liang *et al*., *J. Membr. Sci*., **734**, 124451 (2025), https://doi.org/10.1016/j.memsci.2025.124451
[93] X. Liu, H. Zheng, Q. Chen, J. Ding, K. Huang *et al*., *CIESC J*., **76**, 2294 (2025), https://doi.org/10.11949/0438-1157.20241217
[94] M. J. G. Guimarey, M. A. Marcos, J. P. Vallejo, J. L. Viesca, M. J. P. Comuñas *et al*., *Cellulose*, **31**, 10879 (2024), https://doi.org/10.1007/s10570-024-06181-4
[95] Y. Zhang, S. Fan, W. Hu and J. Li, *Ind. Crop. Prod*., **222**, 119588 (2024), https://doi.org/10.1016/j.indcrop.2024.119588
[96] Y. Cheng, Y. Meng, M. Guan, Y. Cai and X. Liu, *Tribol. Int*., **212**, 110959 (2025), https://doi.org/10.1016/j.triboint.2025.110959
[97] P. Samyn and P. Cosemans, *Polymers*, **16**, 1095 (2024), https://doi.org/10.3390/polym16081095